Energy Conversion and Management: X 27 (2025) 101074

Contents lists available at ScienceDirect

Energy Conversion and Management: X

journal homepage: www.sciencedirect.com/journal/energy-conversion-and-management-x

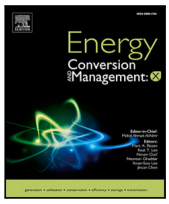

Optimal scheduling of district heat pumps conceived for implementation in Energy Management Systems to participate in demand response

Roberto Rocca [a,b,*], Stefano Leonori [c], Gregorio Fernández Aznar [a], Riccardo Toffanin [d], Luis Luengo-Baranguan [a]

[a] Department of Electrical Systems, CIRCE Technology Centre, Zaragoza, Spain
[b] ENERGAIA Mixed Research Institute (CIRCE Technology Centre and University of Zaragoza), Zaragoza, Spain
[c] Department of Information Engineering, Electronics and Telecommunications (DIET), "Sapienza" University of Rome, Rome, Italy
[d] Azienda Elettrica di Massagno (AEM), Massagno, Switzerland

ARTICLE INFO

Keywords:
Direct demand response
District heating
Energy management system
Flexibility
Heat pump
Indirect demand response
Optimisation

ABSTRACT

Nowadays, the exponential growth of Indirect Demand Response (IDR) and Direct Demand Response (DDR) programs is urging researchers to investigate new strategies to enable the provision of flexibility services from any type of energy device. In the case of Heat Pumps (HPs), research efforts revolve around their integration in Energy Management Systems (EMS). To this end, this work proposes a novel formulation of the optimal scheduling problem of district-level HPs, conceived for EMS implementation, and based on a quadratic programming algorithm, with a specific objective function for IDR and DDR. Furthermore, a rigorous methodology is defined to assess HPs' performance under both IDR and DDR, where IDR price signals pursue a peak-shaving/valley-filling objective, while DDR considers participation in flexibility markets. The proposed optimal scheduling is implemented in a practical case study, based on real data from the Horizon-Europe project REEFLEX. Results under IDR prove the peak shaving and valley filling capabilities, obtaining reductions in consumption peak and peak-to-dip gap of up to 13% and 34% respectively. Possibility of designing IDR price signals to avoid extra costs for the end users is also proven. For DDR, a sensitivity analysis of peak and average consumption against the price of the flexibility offer is conducted. Peak and average consumption are proven to reduce up to 20% and 35% for upwards flexibility, and to increase up to 100% and 80% for downwards flexibility. Besides, the total energy cost increases against the flexibility price offers at rates of up to 3.75% and 11.25%, respectively in upwards and downwards flexibility.

1. Introduction

1.1. Research context and background

Nowadays, an energy transition is ongoing with the ambitious goal of a fully-decarbonised economy by 2050 [1]. In order to tackle the challenges that the transition is posing on the electrical system [2,3], huge research efforts currently revolve around three main fields, namely: installation of energy storage systems [4–6], novel controls in Renewable Energy Sources (RESs) power converters [7,8] and Demand Response (DR).

In DR, consumers are sent signals offering monetary remunerations in return for a change in their expected energy consumption [9]. By responding to these signals, consumers provide grid operators with the so-called flexibility services, such as frequency services, grid stability or congestion management [10]. Based on the type of signal, two types of DR are distinguished: Indirect Demand Response (IDR) and Direct Demand Response (DDR). IDR is conceived to provide services on a continuous basis by means of time-varying tariff signals, which are aimed at shifting electricity use to times of lower demand and/or higher availability of renewable sources [11,12]. Besides, DDR is conceived to provide services on a single-event basis through one-shot incentive signals. In many countries, including the EU, DDR signals cannot be sent directly from grid operators to customers, as they ought to be under market regulation [13]. Consequently, DDR signals are emitted after a trading process, which undergoes in the so-called Flexibility Markets (FMs) [14].

Fostered by the revenue streams offered by flexibility services, DR programs are undergoing an exponential growth, which, in turn, is opening new research pathways focused on the provision of flexibility services through any type of energy device. In this context,

* Department of Electrical Systems, CIRCE Technology Centre, Zaragoza, Spain.
E-mail address: roberto.rocca@ieee.org (R. Rocca).

https://doi.org/10.1016/j.ecmx.2025.101074
Received 24 March 2025; Received in revised form 12 May 2025; Accepted 18 May 2025
Available online 6 June 2025

List of Acronyms

AC	Absorption Chiller
BESS	Battery Energy Storage System
BL	Boiler
CC	Condensation Chiller
CHPS	Combined Heat and Power System
CoP	Coefficient of Performance
DDR	Direct Demand Response
DG	Diesel Generator
DHS	District Heating System
DP	Dynamic Programming
DR	Demand Response
DSO	Distribution System Operator
DT	Dynamic Tariff
EH	Electric Heater
EMS	Energy Management System
EV	Electric Vehicle
FM	Flexibility Market
FT	Flat Tariff
HP	Heat Pump
ICE	Internal Combustion Engine
IDR	Indirect Demand Response
KPI	Key Performance Indicator
LP	Linear Programming
MILP	Mixed Integer Linear Programming
MINLP	Mixed Integer Non-Linear Programming
OF	Objective Function
PV	Photovoltaic
QP	Quadratic Programming
RB	Rule-Based
RES	Renewable Energy Source
SC	Sector Coupling
STC	Solar Thermal Collector
T-PV	Thermal-Photovoltaic
TEC	Total Electricity Cost
TESS	Thermal Energy Storage System
ToU	Time of Use
WT	Wind Turbine

List of Symbols

Δt	time-step duration
λ	IDR pricing function
μ^{HP}	heat pump water mass flow
μ^{mix}	mix valve tapped cold-water mass flow
μ^{us}	users water mass flow
$\boldsymbol{\Phi}^{HP}$	heat pump flexibility
π^{el}	price signal
φ^{FM}	flexibility type boolean parameter
A^{tk}	tank heat exchanging surface
$a_1, \ldots, a_6$	heat pump CoP interpolation coefficients
b^{FM}	flexibility price offer
c^{el}	electricity cost function
c^{FM}	flexibility market window closing time-step
c_p	water specific heat
CoP	heat pump coefficient of performance
E^{HP}	heat pump electric energy absorbed
m^{tk}	tank hot-water mass
N	number of time-steps within the observed time horizon
o^{FM}	flexibility market window opening time-step
P^{DG}	distribution grid total aggregated load
$Q^{HP,rat}$	heat pump thermal power in rated conditions
s^{FM}	flexibility market savings cost function
T^{amb}	ambient temperature
$T^{HP,M}$	heat pump hot-water outlet temperature upper limit
$T^{HP,m}$	heat pump hot-water outlet temperature lower limit
T^{HP}	heat pump hot-water outlet temperature
T^{ret}	cold-water return temperature
$T^{tk,M}$	tank temperature upper limit
$T^{tk,m}$	tank temperature lower limit
T^{tk}	tank temperature
T^{us}	hot-water delivery temperature
$U^{HP,rat}$	heat pump thermal energy produced in rated conditions
U^{HP}	heat pump thermal energy produced
U^{loss}	tank thermal losses
u^{tk}	tank heat exchange factor
X^{HP}	heat pump decisional variable

Sector Coupling (SC) is being heavily investigated [15,16]. SC can be defined as the simultaneous and coordinated optimisation of different energy sectors, with the objective of optimally shifting energy between one another [17]. In particular, great efforts revolve around SC between electricity and urban heating, due to the fact that space heating and hot water production currently account for almost half of the global energy demand in buildings [18], but nearly two thirds of this energy still relies on fossil fuels [19]. As pointed out in [20], heating is an inherently flexible sector, thanks to: (i) the low losses and costs of Thermal Energy Storage Systems (TESSs), and (2) the tolerance of human comfort to broad temperature ranges, which allows heating systems to be modulated within wide ranges of operating points. Consequently, the progressive electrification of urban heating systems is expected to unlock a vast potential for the provision of flexibility services [21].

In the electricity with urban heating SC, flexibility services can be provided by two classes of heat-producing units: Combined Heat and Power Systems (CHPSs) [22] and Heat Pumps (HPs) [23], although DR participation with a biomass-based District Heating System (DHS) has been also analysed [24]. In CHPSs, flexibility provision can be obtained by energy management strategies optimising the share between electricity and heat generated for a given amount of primary energy (oil, gas, etc.). On the other hand, in HP applications, flexibility-oriented energy management strategies are aimed at optimally shifting in time and/or modulating in intensity the electricity absorbed to produce hot water, which needs to be stored in TESSs [25], or hot air, using buildings' thermal inertia itself as a TESS [26].

In general terms, in any energy system, optimal energy management tasks are conducted by an Energy Management System (EMS), i.e., a device that monitors and optimises in near-real-time the scheduling of generation, consumption and storage [27]. Scheduling optimisation, in turn, requires the formulation of an optimisation problem. To this end, all system components need to be modelled through a set of equations and inequalities, which define the optimisation constraints, and a specific cost function has to be defined, e.g., minimum total

operating costs, etc. By keeping the focus on HP-based energy systems for electricity and urban heating SC, all the above yields the critical observation that in order to provide flexibility services with a HP, this last needs to be included in an EMS and its corresponding optimal scheduling problem formulated. In the current state of the art, HP inclusion in EMSs responding to DR signals deeply differs between large-scale, district-level units and small-scale, user-level units. In fact, when it comes to flexibility services provision, district-level systems ensure high availability and easily predictable responses, since only one DR signal is sent to one HP unit, rated from few to several Megawatts, which normally operates on a continuous basis and whose response is simply charging/discharging a large TESS. Conversely, user-level systems require an aggregation process to reach the minimum power threshold needed for service provision, with the additional challenge that HPs availability is subject to user-related factors, such as occupancy ("being at home"), or willingness to tolerate potential comfort risks if flexibility provision requires pre-heating living spaces [28].

1.2. EMSs-oriented HPs optimal scheduling literature review

1.2.1. District-level HPs

Concerning district-level HPs, literature contributions span several aspects, such as optimal control [29], integration in DHSs [30], along with optimal scheduling for implementation in EMSs.

In this regard, Bahlawan [31] tackles the optimal scheduling of a multi-generation system, where a HP is included together with Photovoltaic (PV) panels, a Battery Energy Storage System (BESS), a CHPS, a TESS and Electric Vehicle (EV) chargers. The proposed algorithm is of the Mixed Integer Linear Programming (MILP) type, whose Objective Function (OF) minimises either primary energy consumption or operating costs. Regarding the HP modelling, a piecewise-linear Coefficient of Performance (CoP) function is considered. Participation in an IDR program is accounted for through a Time of Use (ToU) tariff.

In [32], the same Author proposes the use of Dynamic Programming (DP) to optimise the energy and economic scheduling of a university campus energy plant composed of PVs, Solar Thermal Collectors (STCs), CHPS, Boiler (BL), Condensation Chiller (CC), Absorption Chiller (AC), an air-to water and a water-to-water HP, modelled with an unspecified nonlinear CoP model. IDR considers an hourly electricity price signal, based on the Italian energy market.

Ayele [33], proposes an EMS dealing with integrated heat and electricity distribution networks, where one HP is included together with a Boiler (BL), TESS, CHPS and a Wind Turbine (WT). The optimal scheduling problem is based on an evolutionary algorithm, whose OF minimises the operating costs under a Dynamic Tariff (DT) scheme. In terms of HP modelling, a constant CoP is considered.

Bischi [34], presents a data-driven MILP model for the short-term scheduling problem minimising the operating cost of a combined cooling, heating and power system of an industrial facility in Northern Italy. The energy system considered is composed of CHPS, HP, BL, CC, AC and a TESS. HP is modelled with a piecewise-linear function for the CoP. An IDR scheme is considered, based on a ToU tariff.

Zhang [35], explores feasibility and benefits of using district-level HPs for reserve services provision. To this end, a MILP model is developed for the day-ahead scheduling of an electricity and heating system comprising HP, modelled with a constant CoP, BESS and TESS. As reserve provision is tackled, no DR mechanisms are considered.

Moretti [36], proposes an efficient robust optimisation model for the scheduling of a multi-energy systems composed of Diesel Generator (DG), CHPS, BL, PV, BESS, TESS and HP, this last modelled with a piecewise-linear CoP. Optimisation is based on a combination of piecewise linear decision rules and MILP to minimise total operational costs. Hourly electricity prices are considered, based on the Italian energy market.

In [37], the same Author presents a MILP and a Mixed Integer Non-Linear Programming (MINLP) model for the optimal scheduling of multi-energy systems accounting for delivery temperature of units, topology and non-isothermal mixing. The idea is implemented in a system case study composed of BL, HP, TESS, Internal Combustion Engine (ICE), and STC, although excluding DR mechanisms. HP's CoP is modelled through a linear function.

Ghilardi [38], proposes an integrated approach for an EMS, where dynamic thermal energy balance of buildings is included in a MILP optimal scheduling problem to exploit buildings' thermal inertia to increase operational flexibility. The method is applied for total operating costs minimisation in different case study energy systems, counting with BL, CC, HP, PVs and STCs installed at users' level. IDR is considered, based on a ToU tariff. HP is modelled with a piecewise-linear CoP function.

Finally, Wang [39] proposes a Rule-Based (RB) EMS to enhance wind power accommodation through the optimal scheduling of Heat Pumps, Thermal Energy Storage Systems and Combined Heat and Power Systems. The idea is applied in the real case study of Jilin Province, China, simulated with the EnergyPRO software package [40]. HPs CoP is modelled with a piecewise-nonlinear function. DR mechanisms are not considered.

1.2.2. User-level HPs

Apart from district-level HPs, contributions concerned with user-level HPs are also surveyed to complete the overview on the current state of the art.

Simonetti [41], tackles the optimal scheduling of a single-family house, considering three different solar-assisted HP architectures integrated with BESS, TESS, PVs and Thermal-Photovoltaic (T-PV) panels. In this case, a MILP optimisation problem is formulated, minimising the total operating costs, with no participation in DR.

Langer [42], proposes another MILP-based optimal scheduling algorithm for the EMS of a building equipped with a HP, PV, BESS and TESS. Here, the optimisation aims at maximising net profit, self-consumption and self-sufficiency, with no participation in DR.

Salpakari [43], investigates two approaches for minimising the operating costs of a building, a Rule-Based (RB) and a DP-based EMS. In both cases, scheduling of a HP, a PV, two Electric Heaters (EHs) and a TESS is optimised considering a spot-market-based electricity price signal.

In [44], the same Author proposes an optimal scheduling algorithm aimed at studying the economic and grid interaction benefits of HPs, EVs and PVs installed in various households of a residential microgrid, using a Linear Programming (LP) formulation. Once again, the optimisation algorithm is aimed at minimising the operating costs considering a spot-market-based price signal.

Dengiz [45] and Clauss [46], develop two RB EMSs. The first contribution modulates the domestic HPs of a small neighbourhood, where all households are equipped with a PV and a TESS. Optimisation objective is to minimise the heating costs and the surplus energy, with HPs power being modulated in accordance with a spot-market-based price signal. The second work accounts for a single-family detached house equipped with a HP, STC and TESS. In this case, the objectives of heating costs minimisation, as well as reduction in heating use in peak hours are pursued. For the first, a spot-market-based price signal is considered. For the second, a DDR scheme is implemented, although the triggering signal is the heat demand value itself.

In [47], Wu propose a MILP-based scheduling minimising the total energy costs in residential multi-energy systems incorporating electricity, thermal energy, natural gas, and renewable energy, under a three-level ToU electricity price signal.

Efkarpidis, [48], proposes a RB EMS for the optimal day-to-day operation of a typical Greek single-family building consisting of HPs, STCs, PVs, as well as BESS and TESS units. Optimisation is aimed at self-consumption maximisation under a ToU scheme, with rules defined to include priorities on BESS and TESS charging.

Finally, Zhang [49] proposes a MILP-based optimal scheduling of residential HPs and BESSs to provide flexibility services to distribution networks. In this case, remuneration is bounded to following a time-varying signal instructed by the DSO, containing a reserve power reference.

Table 1
Literature review on EMSs-oriented optimal scheduling of energy systems including HPs.

Author	Ref.	Syst. Type	Assets	Algorithm	IDR	DDR
Bahlawan	[31]	District	HP, PV, BES, CHPS, TESS, EV	MILP	ToU	No
Bahlawan	[32]	District	PV, STC, CHPS, BL AC, CC, HP	DP	DT[a]	No
Ayele	[33]	District	HP, BL, TESS, CHPS, WT	Evol.	DT[a]	No
Bischi	[34]	District	CHPS, HP, BL, CC, AC, TESS	MILP	ToU	No
Zhang	[35]	District	HP, BESS, TESS	MILP	No	No
Moretti	[36]	District	DG, CHPS, BL, PV, HP, BESS, TESS,	MILP	DT[a]	No
Moretti	[37]	District	BL, HP, TESS, ICE, STC	MI(N)LP	No	No
Ghilardi	[38]	District	BL, CC, HP, PV, STC	MILP	ToU	No
Wang	[39]	District	CHPS, HP, TESS, BL, WT	RB	No	No
Simonetti	[41]	Domestic	PV, PVT, HP, BESS, TESS	MILP	No	No
Langer	[42]	Domestic	PV, BESS, TESS, HP	MILP	No	No
Salpakari	[43]	Domestic	PV, HP, EH, TESS	RB, DP	DT[a]	No
Salpakari	[44]	Domestic	PV, HP, EV	LP	DT[a]	No
Dengiz	[45]	Domestic	HP, TESS, PV	RB	DT[a]	No
Clauß	[46]	Domestic	STC, HP, TESS	RB	DT[a]	Yes[b]
Wu	[47]	Domestic	CHPS, TESS, HP,PV, EV	MILP	ToU	No
Efkarpidis	[48]	Domestic	BESS, HP, STC, TESS	RB	ToU	No
Zhang	[49]	Domestic	BESS, HP	MILP	ToU+DT[a]	No
This work	**–**	**District**	**HP**	**QP**	**DT[c]**	**Yes[d]**

[a] Based on wholesale market prices.
[b] Based on peak thermal load.
[c] Pursuing peak-shaving/valley-filling objectives.
[d] Based on FM.

Table 2
Technical characteristics of district-level HPs included in surveyed literature.

Author	Ref.	HP type	CoP model
Bahlawan	[31]	Air-to-Water	Piecewise-linear[a]
Bahlawan	[32]	Air-to-Water	Nonlinear (unspec.)
Bahlawan	[32]	Water-to-Water	Nonlinear (unspec.)
Ayele	[33]	Water-to-Water	Constant
Bischi	[34]	Air-to-Water[a]	Piecewise-linear[a]
Zhang	[35]	N.A.	Constant
Moretti	[36]	Air-to-Water[a]	Piecewise-linear[a]
Moretti	[37]	Air-to-Water[a]	Linear
Ghilardi	[38]	Water-to-Water	Piecewise-linear
Wang	[39]	Water-to-Water	Nonlinear (unspec.)
This work	**–**	**Water-to-Water**	**Continuous Quadratic**

[a] Inferred from information available.

1.3. Research contributions

The main outcomes of the above literature survey are summarised in Tables 1 and 2. The former provides an overview of research works related toEMS-oriented optimal scheduling of energy systems including HPs, while the latter adds more technical details about district-level HP considered in the surveyed works. Overall, the main gaps spotted in the current state of the art can be summarised as follows. Firstly, works concerning district HPs optimal scheduling consider large energy systems, counting with several energy assets. To this end, the majority of the surveyed works tends to simplify, i.e., linearise models, with the risk that not all relevant aspects are represented with sufficient accuracy. Secondly, none of the surveyed works, neither on district nor residential HPs, addresses participation in DDR based on FMs. Thirdly, when dealing with Dynamic Tariffs (DTs), the majority of contributions considers spot-market-based prices, which do not pursue the objectives of an IDR program. In fact, spot-market-based tariffs are calculated by matching generation and demand offers, whereas IDR are designed to optimally shift demand in accordance with objectives such as peak-shaving/valley-filling, average load reduction or simultaneity with local renewable generation. In order to fill these gaps spotted in the state of the art, this work wishes to provide a twofold contribution:

1. The formulation of the optimal scheduling problem of large, district-level HPs, conceived for EMSs implementation. The proposed formulation is based on a Quadratic Programming (QP) algorithm, with an OF specifically written for each type of DR. In order to provide a thorough description of the formulation, HP is considered on its own, although with the focus on integrating it with other devices in future works. It is noted that the QP formulation, which opposes linear formulations widely used in the literature, stems from the detailed modelling of the HP system made in this work, reflecting its inherent characteristics. As a consequence, quadratic representation is extended to the CoP.
2. A rigorous assessment of the HP performance in both DR types. In particular, IDR price signals considered pursue a peak-shaving/valley-filling objective, while DDR is based on the operating principle of a FM. Here, it is noted that the proposed assessment methodology is extremely general, and hence easily applicable to any other energy device.

The rest of this paper is structured as follows. Section 2 caters for the optimal scheduling problem formulation of large, district-level HPs. Section 3 outlines the operating principles of the two DR programs and defines their corresponding OFs. Section 4 describes the practical case study considered in this work, whose results are presented and discussed in Section 5.

Research work presented in this paper has been conducted within the framework of the European Project REEFLEX, where both IDR and DDR are considered to assess the potential of various types of energy assets to provide flexibility services and eventually offer them in a newly-developed central service platform and energy marketplace [50].

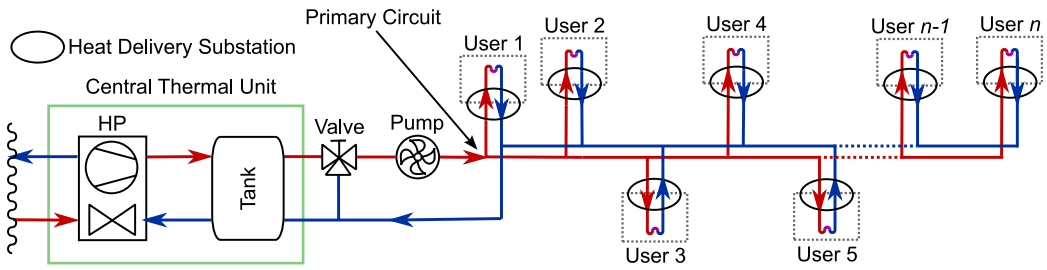

Fig. 1. Simplified example of DHS.

2. District heat pump optimal scheduling problem

This section presents the optimal scheduling problem formulation of district HPs for EMSs implementation. The proposed formulation is developed starting from a DHS architecture composed of a central HP, a TESS, a three-way mixing valve and an aggregated load, as it is sketched in Fig. 1. Before embarking on the problem formulation, the next subsection provides a general overview of the DHS and briefly explains its operating principle.

2.1. District heating systems overview

DHSs are a largely widespread technology, where thermal energy for space heating and domestic hot water is produced in one, or few centralised locations and then distributed to the final users through a piping system [51]. Heat carrier is normally pressurised hot water between 50 °C–90 °C, although lower temperatures are foreseen for the next DHS generation [52]. In line with the architecture considered in this work, the outlook of a DHS having a single central HP, TESS and three-way mixing valve is shown in Fig. 1.

The central HP heats up cold water returning from the users and sends it to a TESS. Then, the "primary" distribution system extracts hot water from the tank and sends it to a three-way valve, where it is mixed with cold water tapped from the return circuit, and finally sent to the users by a pumping system. At the users premises, hot water is delivered either by directly entering users pipes, or through heat exchangers.

It is observed that hot water is usually delivered at a constant temperature, under the control action of the three-way valve. At any time users change their demand, the valve regulates the amount of tapped cold water in such a way as to ensure a constant delivery temperature. In this way, the valve provides fast-response control of the delivery temperature, while leaving it decoupled from that contained in the tank. This, in turn, allows the HP to produce hot water at a variable temperature independently of the users demand, leaving so a considerable degree of freedom for energy management strategies responding to DR signals.

2.2. Notation

In the rest of this work, the following notation is used. A generic quantity is indicated with A^j, where superscript j provides additional information, such as the corresponding component. Then, subscript k is added, A^j_k, to specify the value of A in a generic time step k. For constant quantities, subscript k is omitted.

2.3. Modelling hypotheses

As mentioned in the Introduction, EMSs are aimed at optimising systems energy flows in near-real-time. To do so, the optimal scheduling problem is solved recurrently with frequencies ranging between fifteen to sixty minutes. For this reason, the mathematical modelling needs to ensure a convenient trade-off between accuracy and computation burden. Indeed, over-simplified model would cater for inaccurate results, whereas an over-complicated model might require computation times incompatible with the rest of the system. Based on that, the problem formulation proposed in this work is based on the following simplifying hypotheses:

1. All users are modelled in a unique aggregated load, which includes the pipes losses.
2. The control system is ideal.
3. Water mix inside the tank is instantaneous and thermal stratification is negligible. As discussed in [43], this is a conservative hypothesis for EMS applications.
4. Tank is used as a "buffer", meaning that hot water level is constant.
5. Thermal inertia of all metal parts is negligible.
6. Temperature of the ambient surrounding the tank, T^{amb}, is constant.
7. Cold water return temperature, T^{ret}, is constant, fixed by the pump controller [53].
8. Users hot-water temperature, T^{us}, is constant, controlled by the mixing valve.

Further to the introduction of the above hypotheses, the DHS scheme of Fig. 1 simplifies in the model in Fig. 2, where energy flows are shown in red, along with components temperatures (T^j) and mass flow rates (μ^j).

2.4. Optimisation problem formulation

As shown in Fig. 2, the EMS receives a DR signal and provides the HP with a power/energy control signal, which is obtained by the optimal scheduling problem discussed in the following.

A discrete-time approach is chosen, with time steps ranging from 1 to N, where N represents the total number of time steps within the observed time horizon. All time steps have the same duration Δt.

During each time step, for the generic component j, thermal and electric energies, U^j_k and E^j_k respectively, are given by $U^j_k = Q^j_k \Delta t$ and $E^j_k = P^j_k \Delta t$. In particular, Q^j_k and P^j_k denote the thermal and electric powers. As it is common practice in EMS applications, all powers are assumed as constants during Δt.

Besides, aggregated mass flows μ^j_k are equal to $\dot{m}^j_k \Delta t$, where $\dot{m}^j_k$ indicates the mass flow rate. As done for powers, mass flow rates are assumed as constant during Δt. Finally, temperatures T^j_k are also assumed as constants during Δt.

In the following, equations and inequalities describing the operation of each component are written, defining the constraints of the optimisation problem.

2.4.1. Users

In the proposed model, users are represented as a heat-absorbing component. For a given thermal energy demand profile U^{us}_k, its mathematical expression is given by:

$$U^{us}_k = \mu^{us}_k c_p (T^{us} - T^{ret}), \tag{1}$$

where μ^{us}_k is the corresponding mass flow.

As it can be noted, provided that U^{us}_k is an input for the EMS, while T^{us} and T^{ret} are known, μ^{us}_k can be calculated directly from (1).

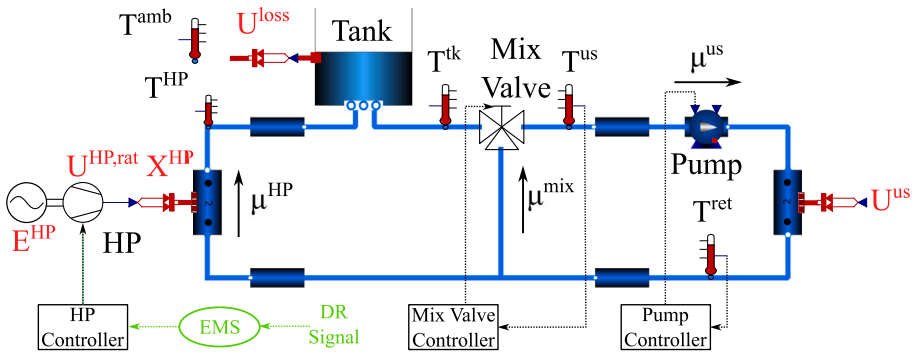

Fig. 2. Simplified HP-based DHS model overview.

2.4.2. Heat pump

The HP is modelled as a heat-generating component, which elaborates the aggregated mass flow μ_k^{HP} returning from the users and heats it up to T_k^{HP} by providing the thermal energy U_k^{HP}:

$$U_k^{HP} = \mu_k^{HP} c_p \left(T_k^{HP} - T^{ret}\right). \tag{2}$$

U_k^{HP}, in turn, is produced from the electric energy E_k^{HP} in a vapour-compression cycle characterised by a variable CoP_k. In this work, the control variable selected is X_k^{HP}, representing the thermal energy provided by the HP expressed in per-unit, which is defined by:

$$E_k^{HP} = \frac{U_k^{HP}}{CoP_k} = X_k^{HP} U^{HP,rat} CoP_k^{(-1)}, \tag{3}$$

where X_k^{HP} is subject to:

$$0 \le X_k^{HP} \le 1. \tag{4}$$

In (3), $U^{HP,rat}$ indicates the thermal energy that the HP can provide by operating at rated power during Δt. Furthermore, the inverse of CoP_k is expressed as a function of X_k^{HP} and T_k^{HP} through a second-order polynomial:

$$\begin{aligned} CoP_k^{(-1)}(T_k^{HP}, X_k^{HP}) = {} & a_1 (T_k^{HP})^2 + a_2 T_k^{HP} X_k^{HP} + a_3 (X_k^{HP})^2 + \\ & + a_4 T_k^{HP} + a_5 X_k^{HP} + a_6. \end{aligned} \tag{5}$$

In the approach followed in this work, polynomial coefficients are obtained by interpolating a set of experimental data. Choice of a second-order polynomial is analysed in Appendix A.

2.4.3. Tank

The tank, having mass m^{tk}, represents the TESS of the system. Its temperature T_k^{tk} can be expressed thanks to the energy balance equation:

$$T_k^{tk} = \frac{X_k^{HP} U^{HP,rat} - U_k^{loss} - U_k^{us}}{m^{tk} c_p} + T_{k-1}^{tk}, \tag{6}$$

where T_k^{tk} is subject to:

$$T^{tk,m} \le T_k^{tk} \le T^{tk,M}. \tag{7}$$

As it can be noted, T_k^{tk} is an indicator of the energy available within the system, as its value is a function of T_{k-1}^{tk}. Therefore, T_k^{tk} represents a system's state variable.

In (6), U_k^{loss} represents the tank heat losses. Provided that A^{tk} is the tank heat-exchanging surface, u^{tk} the exchange factor and T^{amb} the ambient temperature, U_k^{loss} can be expressed as:

$$U_k^{loss} = u^{tk} A^{tk} (T_k^{tk} - T^{amb}) \Delta t. \tag{8}$$

2.4.4. Mix valve

As discussed in Section 2.1, the three-way valve mixes hot water extracted from the tank with cold water tapped from the return pipe. Reminding that the mass flow extracted from the tank is equal to μ_k^{HP} (see hypothesis 4), mass flow balance can be expressed as:

$$\mu_k^{HP} + \mu_k^{mix} = \mu_k^{us}, \tag{9}$$

where μ_k^{mix} is the mass flow tapped from the return pipe.

Subsequently, reminding that T^{ret} and T^{us} are constants (see hypotheses 7 and 8), energy conservation equation can be written as:

$$\mu_k^{HP} c_p T_k^{tk} + \mu_k^{mix} c_p T^{ret} = \mu_k^{us} c_p T^{us}. \tag{10}$$

Thanks to (9) and (10), T_k^{HP} can be expressed directly as a function of the control and state variables, X_k^{HP} and T_k^{tk} respectively, as:

$$T_k^{HP} = \frac{X_k^{HP} U^{HP,rat}}{U_k^{us}} \left(T_k^{tk} - T^{ret}\right) + T^{ret}, \tag{11}$$

with T_k^{HP} subject to:

$$T^{HP,m} \le T_k^{HP} \le T^{HP,M}. \tag{12}$$

Full derivation of (11) is presented in Appendix B.

3. Demand response programs, operating principle and objective function

Regarding the cost function chosen for the OF formulation, it is defined in this work depending on the type of DR program, as shown in the following.

3.1. Indirect demand response

As discussed in the Introduction, IDR is a mechanism conceived for managing electricity demand by influencing consumers behaviour through price signals, which are specifically designed to alleviate stress on distribution grid and/or incentives use of local renewable energy, by pursuing objectives such as peak shaving, valley filling, ToU, etc.

This works takes into account the objective of alleviating stress on distribution grids. To properly define the IDR price signals, the quantity P_k^{DG} is introduced, which is defined as the aggregated load at the kth instant of all users connected to a given distribution grid. In other terms, P_k^{DG} is chosen as a representative indicator of the stress level in the distribution grid.

The general approach to obtain the IDR price signal $\pi_k^{el,IDR}$ is based on the definition of a function λ_k, expressing $\pi_k^{el,IDR}$ as a function of P_k^{DG}:

$$\pi_k^{el,IDR} = \lambda_k \left(P_k^{DG}\right). \tag{13}$$

Concerning λ_k, two observation can be made:

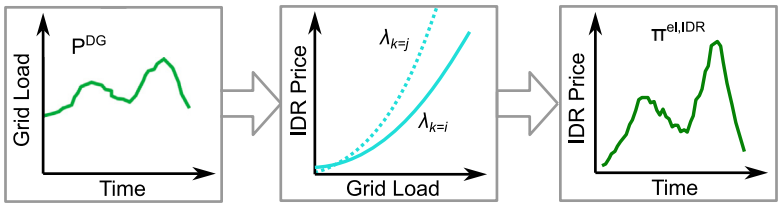

Fig. 3. IDR price signal generation from aggregated distribution grid load. Example of λ function is given in two time steps, i and j.

1. it is a monotonically increasing function, since higher prices are usually applied to high values of P_k^{DG} to incentivise a lower consumption and thus alleviate the stress in the grid;
2. its evaluation is based on the concept of demand price elasticity, i.e., the responsiveness of the electricity demand to a change in price. Reminding that elasticity can change over time, in order to maintain the highest level of generality possible, λ_k has been expressed in terms of the kth time step. An example of the process to evaluate λ_k from the definition of price elasticity is provided in [54].

Fig. 3 illustrates the process to determine the IDR price signal, together with an example of the shape of λ_k. As it can be seen, at any time step, for each value of P_k^{DG} the corresponding price $\pi_k^{el,IDR}$ is found through λ_k.

Once the IDR price signal is determined, the OF can be formulated. In this work, the Total Electricity Cost (TEC), indicated as TEC^{IDR}, is chosen. Following from the definition of $\pi_k^{el,IDR}$, TEC^{IDR} is obtained by minimising a single cost function, i.e., $c^{el,IDR}$, which is equal to:

$$TEC^{IDR} = \sum_{k=1}^{N} c_k^{el,IDR} = \sum_{k=1}^{N} E_k^{HP} \pi_k^{el,IDR}. \tag{14}$$

3.2. Direct demand response

As mentioned in the introduction, DDR is conceived to provide flexibility services on a single-event basis, with one-shot incentives being the outcome of a negotiation undergone in a FM. Its operating principle is as follows. When the DSO detects/foresees a technical issue in the distribution grid, such as an outage or an overload, a bidding window is opened in a FM. Then, all customers belonging to the grid area affected by the issue can offer flexibility. In mathematical terms, flexibility Φ_k^{HP} is defined as:

$$\Phi_k^{HP} = E_k^{HP} - E_k^{HP,base}, \tag{15}$$

where E_k^{HP} is the energy consumption profile optimised by the EMS in response to the DR signal, whereas $E_k^{HP,base}$ is the baseline energy consumption profile, i.e., the hypothetical consumption that the consumer would have without participating in the DR action [55].

All FM windows are defined by an opening and closing time step, o^{FM} and c^{FM}. Here, each consumer willing to participate evaluates its flexibility available during the window duration and presents a bid accordingly, which must contain:

1. Amount of flexibility offered, based on (15);
2. Price at which flexibility is offered. The offers prices usually contain two components, one for reserve and one for activation [14]. In order to keep this work at its simplest without losing generality, a unique flexibility offer is considered b^{FM}, comprising the two components.

Analogously to the IDR, the OF to minimise is TEC^{DDR}, which is obtained by minimising the difference between two cost functions, namely $c^{el,DDR}$ and s^{FM}. Considering a generic case where W FM windows are present within the observed time horizon, it is given by:

$$TEC^{DDR} = \sum_{k=1}^{N} c_k^{el,DDR} - \sum_{w=1}^{W} s_w^{FM}. \tag{16}$$

$c^{el,DDR}$ represents the contribution to the TEC due to consumption E_k^{HP} and price π_k^{el}, bearing in mind that π_k^{el} is totally unrelated to the DR program:

$$c_k^{el,DDR} = E_k^{HP} \pi_k^{el}. \tag{17}$$

The second term represents the savings obtained by participating in the FM. Considering the wth FM window, comprised between o_w^{FM} and c_w^{FM}, s_w^{FM} can be expressed as:

$$s_w^{FM} = \varphi_w^{FM} b_w^{FM} \sum_{k=o_w^{FM}}^{c_w^{FM}} \Phi_k^{HP}. \tag{18}$$

The first, is needed to distinguish between market windows where the requirement is a reduction or an increase in consumption, which are referred to respectively as "upwards" and "downwards" flexibility. To this end, φ_w^{FM} is introduced as a boolean parameters known a priori. In the upwards case, electricity demand is lower than the baseline, so that the flexibility term is negative. In order to keep s_w^{FM} positive, φ_w^{FM} is equal to 1; in the downwards case, to −1:

$$\varphi_w^{FM} = \begin{cases} 1, & if\ FM\ is\ upwards \\ -1, & if\ FM\ is\ downwards. \end{cases} \tag{19}$$

Besides, the second term of (18) contains the flexibility price offered. As it can be seen, it changes for different market windows. Finally, the third term gives the amount of flexibility offered, as defined in (15).

3.3. Remarks and observations

Regarding the optimisation problem complexity, it is now possible to observe that it presents no boolean variables, and that it is quadratic, as it can be seen in (11) where the variable T^{tk} multiplies X^{HP}. In conclusion, the optimisation problem is of the Quadratic Programming (QP) type, and hence can be solved through various software commercially available, such as CVXOPT [56], GAMS [57], or GUROBI [58]. In this work, a Python-GUROBI environment is used.

4. Practical case study

The practical case study considered in this work is based on a DHS counting with a centralised water-to-water HP, which serves a mix of residential and small-business end-users. Table 3 reports the main characteristics of HP and DHS, including tank water mass, HP rated power, as well as allowed components temperature ranges with their respective set-points. For this case study, the following hypotheses have been made:

- As it is common practice in research works focusing on optimal scheduling, in order not to overlap results with forecasting errors, the latter is assumed to be perfect (prediction errors are neglected).
- All time series possess a 15 min granularity.
- IDR price signal and FM opening and closing time signals, are notified to users at least 24 h in advance.

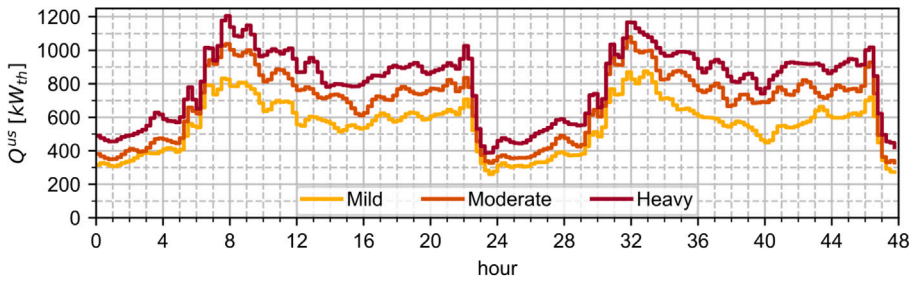

Fig. 4. Heat demand profiles in typical 48-hours for different winter weather conditions.

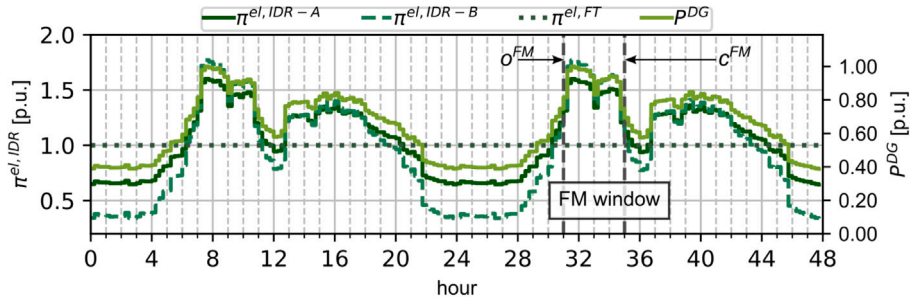

Fig. 5. Electricity tariffs vs. time (left y-axis), and P^{DG} vs. time (right y-axis).

Table 3
Main HP and DHS data.

Quantity	Symbol	Value	Measure unit
Tank mass	m^{tk}	125	[Tons]
HP rated power	$Q^{HP,rat}$	1200	[kW]
HP min–max temperature	$T^{HP,m}$ - $T^{HP,M}$	35–48	[°C]
Users temperature set-point	T^{us}	40	[°C]
Return temperature set-point	T^{ret}	35	[°C]
Tank min–max temperature	$T^{tk,m}$ - $T^{tk,M}$	40.5–48	[°C]

4.1. Input data

Provided that the capability of providing flexibility services with a DHS depends on the amount of thermal energy to be handled, i.e., thermal demand, this work considers three different weather conditions, which are referred to as mild, moderate and heavy. For each of them, a typical 48-hour thermal demand profile, Q^{us}, has been obtained from real data collected from December 2023 to March 2024 within the framework of the REEFLEX Project, in the DHS of Capriasca (Canton Ticino, CH) [59], which serves a small district with a mix of residential and small-business users. The three Q^{us} profiles are plotted in Fig. 4. Based on the above profiles, HP rated power and tank capacity have been selected by following traditional sizing criteria [60].

4.2. Key performance indicators

In order to assess the HP performance in the two DR types, this subsection presents the set of four Key Performance Indicators (KPIs) defined in this work to quantify the improvements obtained by means of the optimisation of the HP scheduling:

1. Peak demand reduction, $\overline{E^{HP,pk}}$, accounting for peak shaving effects:

$$\overline{E^{HP,pk}} = 1 - \frac{\max\left(E_k^{HP}\right)}{\max\left(E_k^{HP,base}\right)}, \quad k = k_a, \ldots, k_b, \tag{20}$$

where k_a and k_b denote two generic time steps, E_k^{HP} and $E_k^{HP,base}$ are the energy consumption under DR and baseline conditions respectively.

2. Peak-to-dip gap reduction, $\overline{E^{HP,pk-dp}}$, accounting for the combination of peak-shaving and valley-filling effects:

$$\overline{E^{HP,pk-dp}} = 1 - \frac{\max\left(E_k^{HP}\right) - \min\left(E_k^{HP}\right)}{\max\left(E_k^{HP,base}\right) - \min\left(E_k^{HP,base}\right)}, \quad k = k_a, \ldots, k_b. \tag{21}$$

3. Average demand reduction, $\overline{E^{HP,avg}}$:

$$\overline{E^{HP,avg}} = 1 - \frac{\sum_{k=k_a}^{k_b} E_k^{HP}}{\sum_{k=k_a}^{k_b} E_k^{HP,base}}. \tag{22}$$

4. Total Electricity cost reduction, $\overline{TEC^{DDR}}$:

$$\overline{TEC^{DR}} = 1 - \frac{TEC^{DR}}{TEC^{base}}. \tag{23}$$

where TEC^{DR} denotes the total electricity cost under IDR, TEC^{IDR}, or DDR, TEC^{DDR}, while TEC^{base} accounts for baseline conditions. As it can be noted, the former coincides with the OF.

4.3. Indirect demand response scenario

In this operating scenario, two different IDR price signals are considered, where the second one imposes a higher penalty to consumption peaks. The objective is indeed to compare the HP performance, as well as to observe the different responses of the EMS under both price signals. Finally, a Flat Tariff (FT) is considered as a term of comparison.

IDR price signals have been obtained by following the process outlined in Section 3.1. In particular, two steps have been followed:

1. Definition of a P^{DG} profile.
2. Definition of a P^{DG} vs. IDR price function λ, as in Section 3.1.

Regarding P^{DG}, the profile considered is that of the distribution network of Capriasca, which serves the same district as the DHS (mix of residential and small-business users). Consistently with the thermal demand, a typical 48-hour profile has been obtained from December

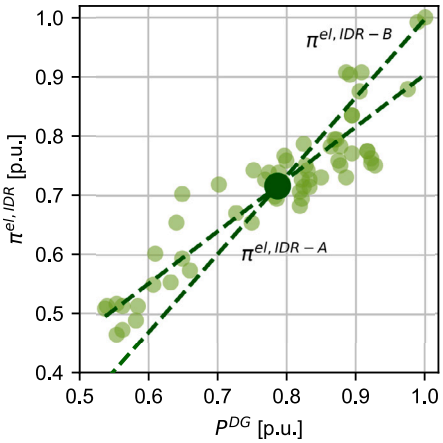

Fig. 6. Normalised grid load level vs. pricing [54].

2023 to March 2024 data, considering real data obtained within the framework of the REEFLEX Project. The profile is shown in Fig. 5 in light green. As it can be seen, the profile is expressed in per unit with respect to the peak value, in order to maintain the highest level of generality possible.

Regarding the definition of λ, the work done in [54] has been considered. From this work, the P^{DG} vs. $\pi^{el,IDR}$ characteristics obtained in a winter case study have been normalised and plotted against each other. The resulting scattered plot is shown in Fig. 6. As a first approximation, it is deemed reasonable to consider λ as a linear function, as well as removing its dependence from the time instant k.

At this point, all inputs required to calculate the IDR price signals are available. Based on that, two $\pi^{el,IDR}$ signals are obtained:

1. $\pi^{el,IDR-A}$, by considering the same slope as in Fig. 6 (IDR-A).
2. $\pi^{el,IDR-B}$, obtained by increasing the slope of $\pi^{el,IDR-A}$ by 20%, while maintaining the same average value (IDR-B).

As mentioned above, the idea with IDR-B is to represent a DR program where a higher penalty is imposed over peak consumption. The FT $\pi^{el,FT}$ is obtained as the average between $\pi^{el,IDR-A}$ and $\pi^{el,IDR-B}$ over the 48 h. It is highlighted that HP performance under $\pi^{el,FT}$ are taken as baseline for the KPIs calculation.

The three IDR price signals are plotted in Fig. 5. Here, it is important to observe that the three signals have been expressed in per unit, with respect to $\pi_k^{el,FT} = 1$ $(k = 1...N)$. This choice has been made in order to maintain the highest level of generality possible and hence results can be easily extended to other district HPs of the same climatic region. Possibility of using per-unit prices is given by two factors:

- All KPIs defined in this case study are already expressed in per unit, so that absolute price values are not necessary.
- Results of the optimisation performed by the EMS do not depend on the scale factor applied to the price signals.

4.4. Direct demand response scenario

In this case, the optimal scheduling algorithm discussed in the previous sections is used to perform a sensitivity analysis where KPIs are evaluated for different values of the offered flexibility prices $b^{FM,a/r}$. To this end, all elements composing (18) need to be defined.

Concerning s^{FM}, in order to maintain the case study at a reasonable level of simplicity without losing generality, the following assumption is introduced that only one market window opens within the observed time horizon.

Table 4
Indirect DR KPIs.

	Mild		Moderate		Heavy	
	$IDR-A$	$IDR-B$	$IDR-A$	$IDR-B$	$IDR-A$	$IDR-B$
$\overline{E^{HP,pk}}$	0.014	0.085	0.026	0.101	0.131	0.114
$\overline{E^{HP,pk-dp}}$	0.017	0.246	0.046	0.324	0.266	0.337
$\overline{E^{HP,avg}}$	−0.019	−0.087	−0.020	−0.067	−0.020	−0.060
$\overline{TEC^{IDR}}$	−0.108	−0.001	−0.111	−0.011	−0.105	−0.002

To evaluate TEC^{DDR}, the same flat tariff used for IDR is taken, in order not to include the effects of a time-varying tariff and thus isolate the effects of the DDR signal.

For the definition of o^{FM} and c^{FM}, the P^{DG} profile of Fig. 5 is once again considered. Considering a day-ahead notification, o^{FM} and c^{FM} are set respectively at 7 AM and 11 AM of the second day, with the goal of alleviating the morning peak demand.

5. Results and discussion

5.1. Indirect demand response

HP performance in IDR is assessed in this subsection for the three weather conditions shown in Fig. 4, considering price signals IDR-A and -B, along with the FT serving as baseline.

5.1.1. EMS energy flows analysis

In order to give an overview of the EMS response, assessment begins by analysing the energy profiles U^{us}, U^{HP}, U^{loss} along with the tank stored energy variation ΔU^{tk} under the three pricing schemes. Due to the relative similarity of results obtained for different weather conditions, in order to maintain the manuscript within a reasonable length, only moderate weather results are plotted in Fig. 7. Additionally, the corresponding HP and tank temperature profiles, T^{HP} and T^{tk}, are plotted in Fig. 8.

As it can be seen in Fig. 7(c), when a FT is applied, the EMS leads the system to minimise the overall energy consumption by minimising the tank charge/discharge cycles and thus keeping T^{tk} at its lowest, as shown in Fig. 8(c). Indeed, apart from an initial discharge made to take advantage of the energy stored in the initial conditions (T^{tk} is initially at 42 °C), extremely small cycles are made in situation where the CoP needs be optimised. By contrast, under IDR, the EMS leads the system to maximise U^{HP} in timesteps of low price, as reflected by the tank charge/discharge cycles respectively in the night/morning hours depicted in Fig. 7(a) and (b). Here, it is important to observe the effects of IDR-B. In the second day, the very low price at night leads to tank to charging from 11 PM to 6 AM, whereas under IDR-A charging begins only at 1:30 AM. The different tank charging/discharging cycles are also reflected in the T^{tk} profiles shown in Fig. 8(a) and (b), where it is possible to note that under IDR-B tank is charged with hot water produced at maximum temperature, i.e., 48 °C, whereas under IDR-A the maximum HP outlet temperature never exceeds 46 °C.

5.1.2. KPIs assessment and analysis

The EMS response conducted above caters for useful insights to assess the KPIs obtained, whose values are reported in Table 4. By observing $\overline{E^{HP,pk}}$ and $\overline{E^{HP,pk-dp}}$, it is possible to note the effectiveness of the IDR program. In fact, beneficial effects in terms of peak shaving and valley filling are obtained with the EMS set to minimise the total electricity cost. In a bid to better understand the results, Fig. 9 shows the HP electric consumption profiles, E^{HP}, under the three pricing schemes in the different weather conditions.

In terms of $\overline{E^{HP,pk}}$, it can be observed that IDR-B results more effective than IDR-A with mild and moderate weather, achieving peak reductions of respectively of 8.5% and 10.1% with respect to a FT. Conversely, with heavy weather conditions, IDR-A features a better

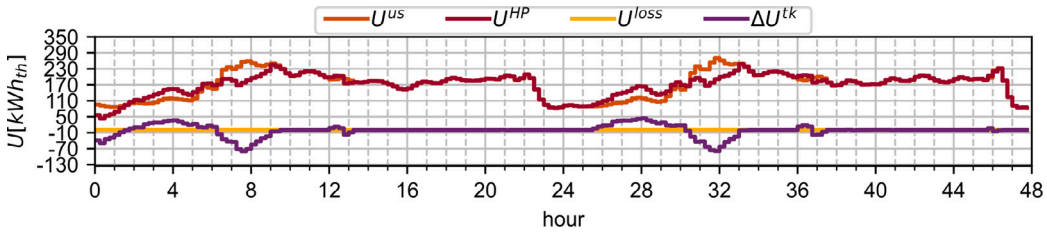

(a) IDR-A

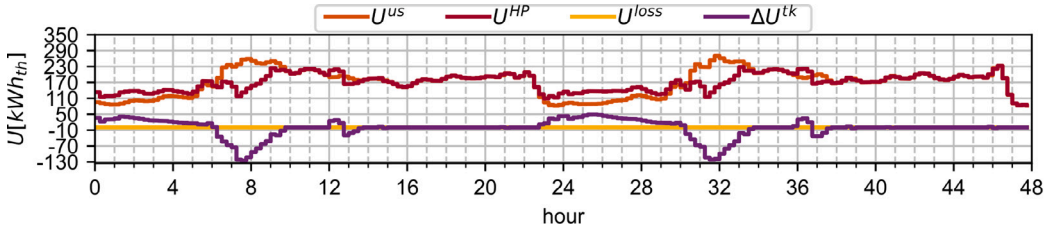

(b) IDR-B

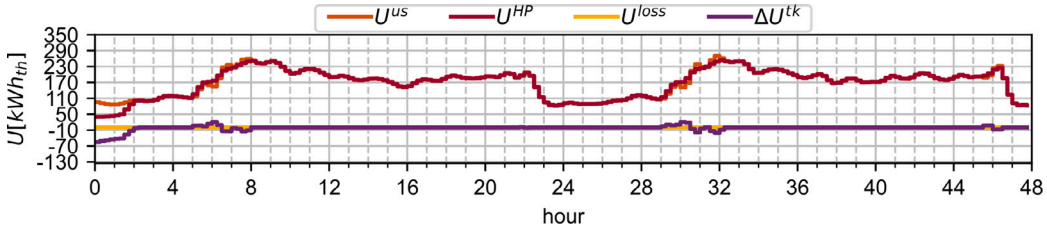

(c) FT

Fig. 7. IDR energy profiles with moderate weather.

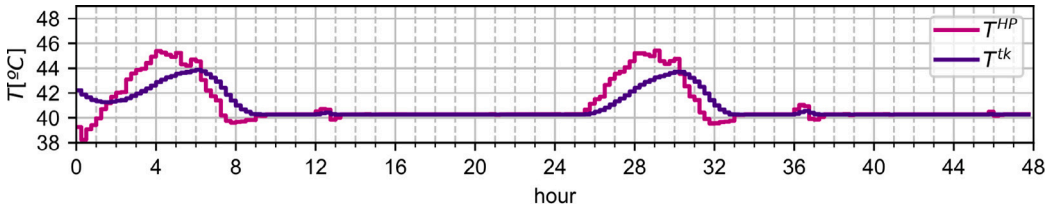

(a) IDR-A

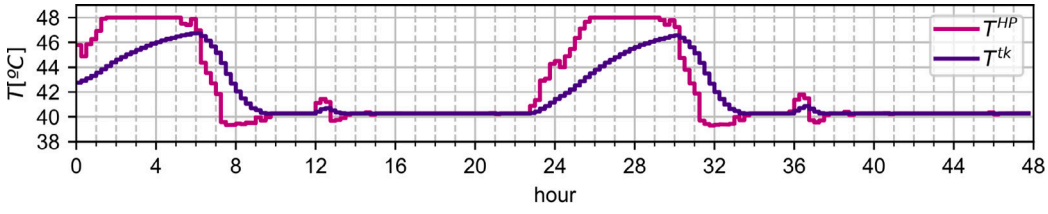

(b) IDR-B

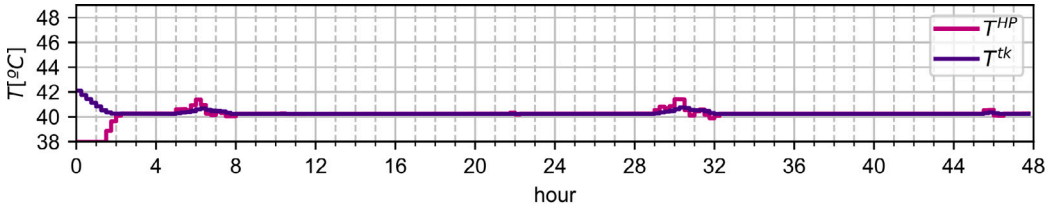

(c) FT

Fig. 8. IDR HP and tank temperatures with moderate weather.

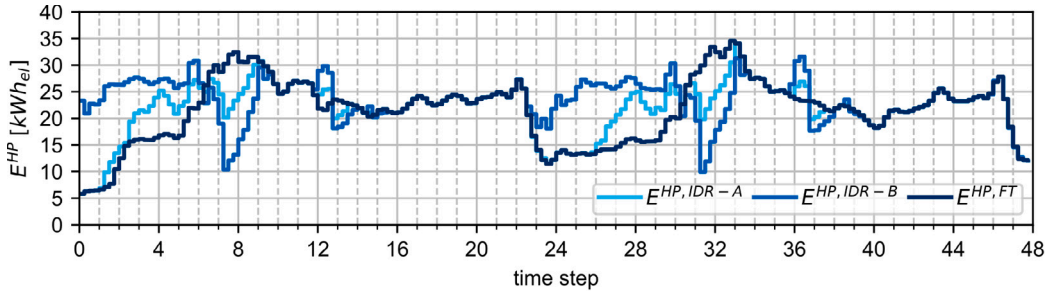

(a) mild weather

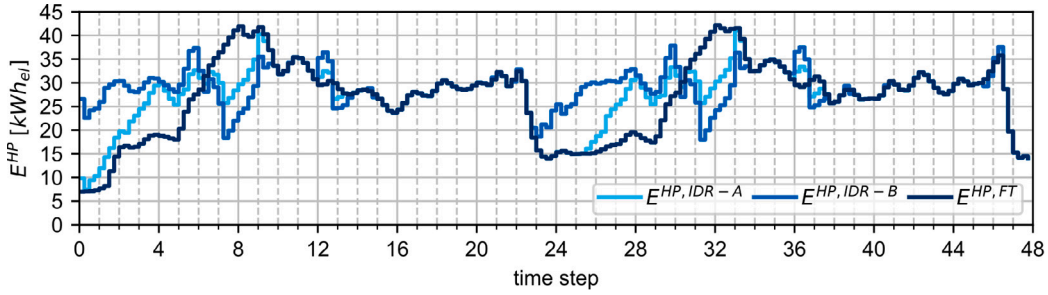

(b) moderate weather

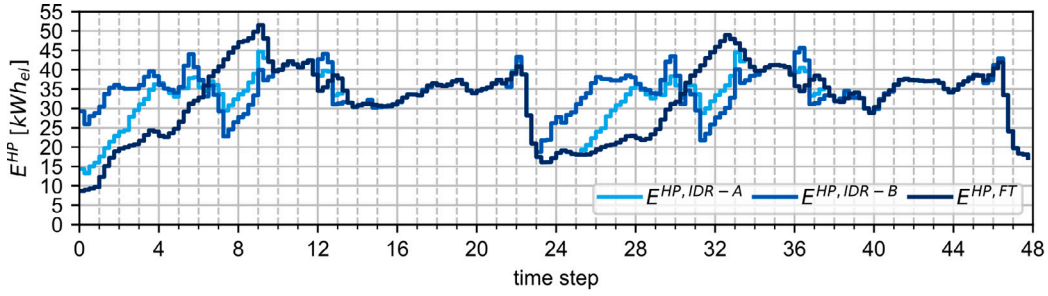

(c) heavy weather

Fig. 9. Indirect DR HP electric consumption profiles.

peak shaving effect, attaining a reduction of 13.1% compared to a FT. This is due to the fact that in heavy weather conditions under IDR-A the EMS response changes, with an earlier tank charging. This, in turn, leads to the elimination of the $E^{HP,IDR-A}$ spike at 9 AM with consequential benefits for $\overline{E^{HP,pk}}$.

By focusing on $\overline{E^{HP,pk-dp}}$, IDR-B provides considerable better results than IDR-A regardless of the weather conditions, reaching an improvement in peak-to-dip gap of 33.7% with respect to a FT. Overall, this behaviour highlights that a major difference between maximum and minimum daily prices leads the EMS to smooth the E^{HP} profile.

The main drawback of providing peak shaving and valley filling services is highlighted by $\overline{E^{HP,avg}}$. As it can be seen in Table 4, the provision of flexibility services yields to a higher average electricity consumption with respect to a FT for both IDR signals. For IDR-A, the increase is of around 2%; for IDR-B, it ranges from 8.7% with mild weather to 6% with heavy weather. The reason lies in the fact that following an IDR price signal leads to an EMS response where the HP works at lower CoPs. This effect can be observed in Fig. 10. Here, the HP operating points are represented as dots in the X^{HP} vs. T^{HP} plane, where a number of iso-CoP curves are plotted. As already observed, under a FT, the EMS forces the HP to operate at its minimum outlet temperature. This behaviour reflects into the "vertical line" at 40.5 °C, which, in turn, corresponds to CoP values between 5.6 and 6.6. Conversely, under IDR, charging the tank at higher HP temperatures leads to operating conditions of lower CoPs, with minima of 5 under IDR-A and 4.6 under IDR-B.

KPIs assessment concludes with $\overline{TEC^{IDR}}$. Here, the main point to note is that IDR-B adds no extra electricity costs for the end-user, whereas under IDR-A costs increase of around 10%. This outcome proves the effectiveness of IDR to provide flexibility services without adding extra costs to the final users, provided that the price signal is designed correctly.

5.2. Direct demand response

This subsection addresses the HP performance in DDR for the three weather conditions shown in Fig. 4. Once again, operation under a FT is taken as baseline condition.

5.2.1. EMS energy flows analysis

In a bid to analyse the response of the EMS to DR signals, assessment begins by analysing the energy profiles U^{us}, U^{HP}, U^{loss} along with the variation in tank stored energy ΔU^{tk}. Once again, in order to provide an insightful overview of the EMS behaviour while keeping the manuscript within a reasonable length, only moderate weather results are analysed. In Fig. 11, subplots show the bespoke energy profiles (it is noted that b^{FM} values are expressed in per unit with respect to the FT, which however is equal to 1). The beginning and the end of

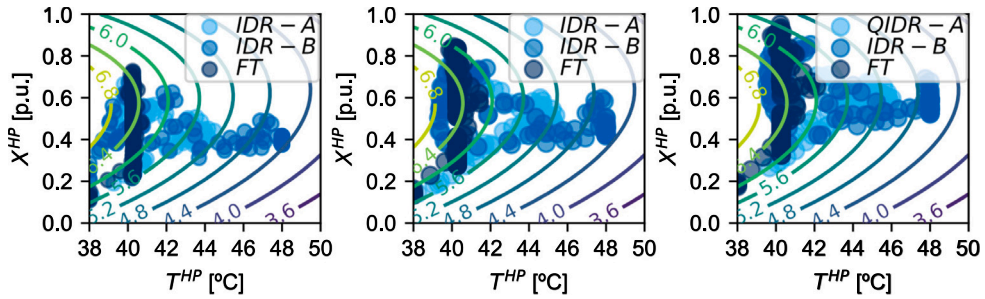

(a) mild weather (b) moderate weather (c) heavy weather

Fig. 10. Indirect DR, HP CoP operating points.

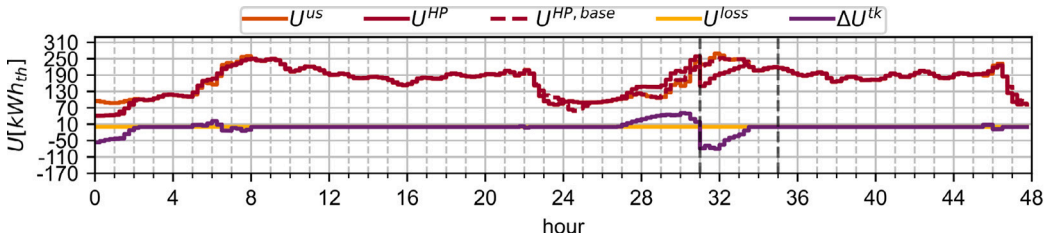

(a) $b^{FM} = 1$, upwards flexibility

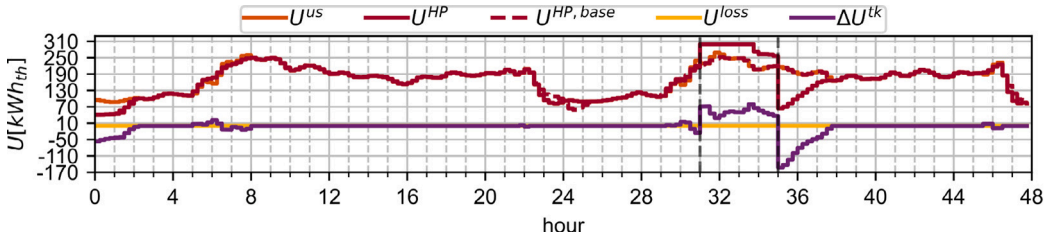

(b) $b^{FM} = 1$, downwards flexibility

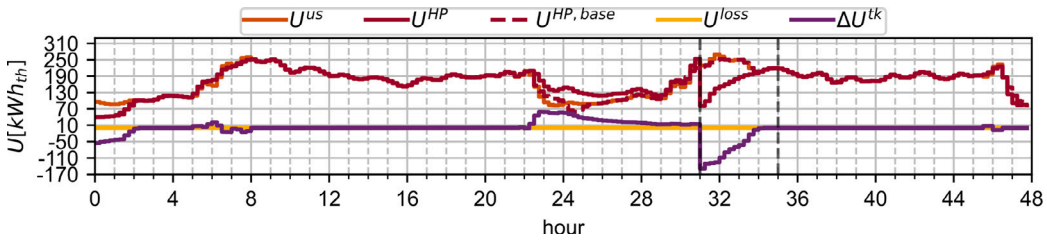

(c) $b^{FM} = 10$, upwards flexibility

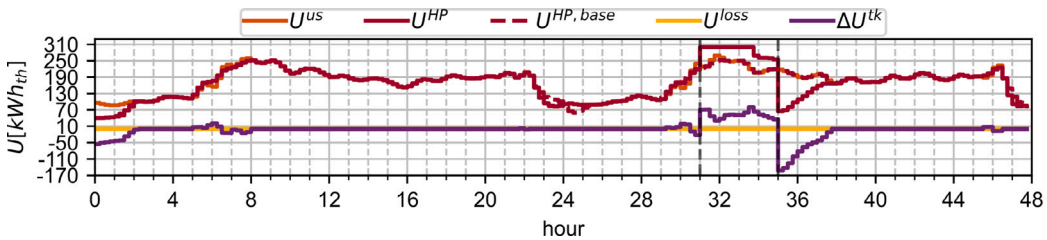

(d) $b^{FM} = 10$ and downwards flexibility

Fig. 11. DDR energy profiles with moderate weather.

the FM window are marked by vertical dashed lines. Besides, Fig. 12 reports the corresponding HP and tank temperature profiles T^{HP} and T^{tk}.

In terms of upwards flexibility (consumption reduction), Fig. 11(a) and (c) show how the tank is pre-charged to reduce consumption during the FM window. Here, the EMS response changes for different flexibility offers. For $b^{FM} = 1$, pre-charge begins at 3 AM, whereas for $b^{FM} = 10$ at 11 PM of the first day. In terms of temperatures, the first b^{FM} condition leads the EMS to respond in such a way that maximum T^{HP} and T^{tk} are never reached, as shown in Fig. 12(a). Conversely, for $b^{FM} = 10$, the maximum HP temperature of 48 °C is reached at midnight and maintained until the beginning of the FM window.

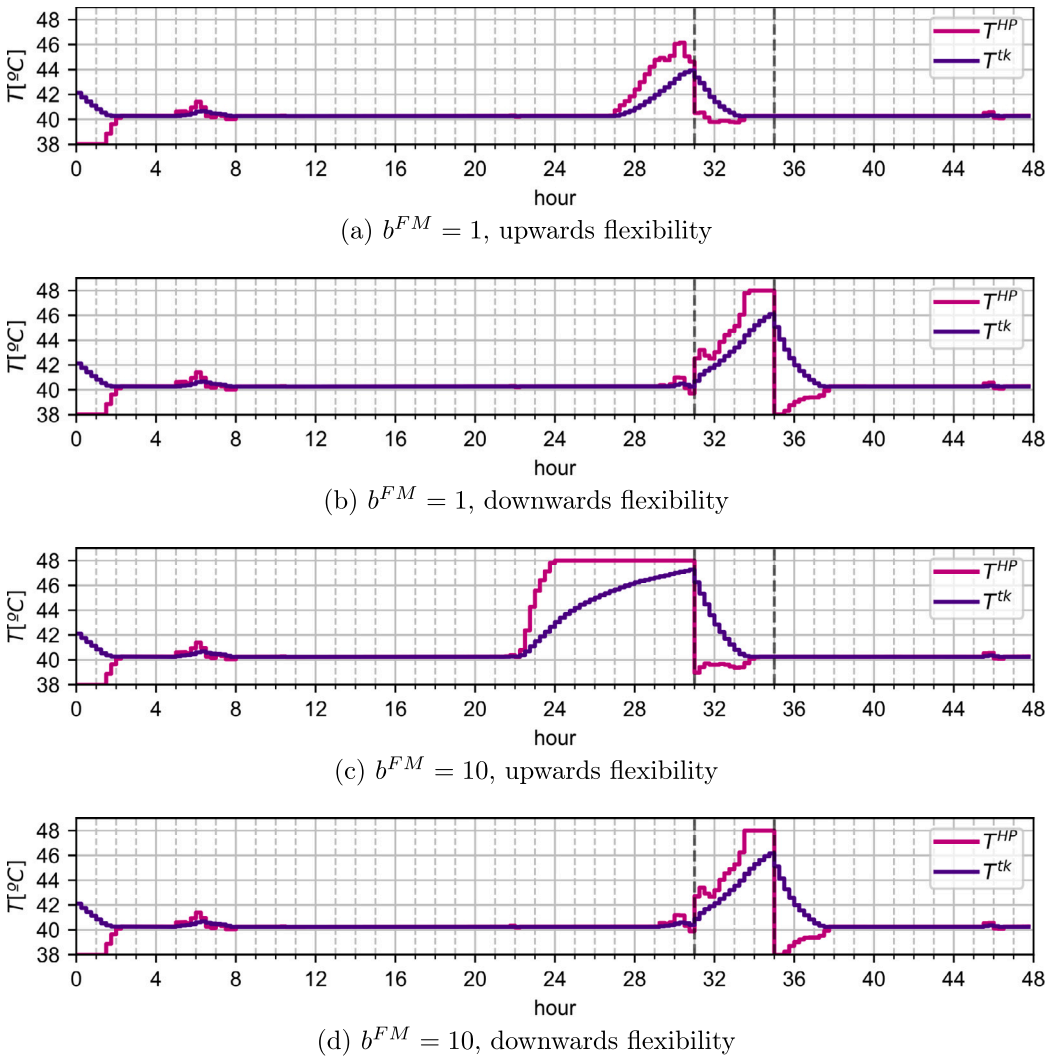

(a) $b^{FM} = 1$, upwards flexibility

(b) $b^{FM} = 1$, downwards flexibility

(c) $b^{FM} = 10$, upwards flexibility

(d) $b^{FM} = 10$, downwards flexibility

Fig. 12. DDR temperature profiles with moderate weather.

By moving now to downwards flexibility (consumption increase), the EMS response is identical for the two values of b^{FM} (see Fig. 11(b) and (d)). This time, the EMS does not commend a tank pre-discharge, as discharge starts soon after the FM window.

As introduced in Section 3.2, the OF in DDR is expressed by (18). Here, savings obtained from participation in FM, s^{FM}, are directly proportional to the amount of flexibility offered, Φ^{HP}. The latter is expressed by (15), highlighting that Φ^{HP} is maximised by: minimising E^{HP} in upwards flexibility, or maximising it in downwards flexibility. To this end, it is of extreme importance to acknowledge the technical factors that limit the amount of Φ^{HP}. In upwards flexibility, limitations are incurred only with $b^{FM} = 10$ during the tank pre-charge, where the HP power is limited by the hot-water temperature limit. Conversely, no limit conditions are incurred during the FM window. In downwards flexibility, two different limits are reached. At the beginning of the FM window, between 7 AM and 9:30 AM, the HP runs at its rated power, as indicated by the flat line of U^{HP}=300kWh_{th} (see Fig. 12(b) and (d)). In the final part of the FM window, i.e., between 9:30 AM and 11 AM, the HP power is curtailed as the maximum hot-water temperature is reached.

5.2.2. KPIs assessment and analysis

KPIs assessment is conducted by means of a sensitivity analysis, where $\overline{E^{HP,pk}}$ and $\overline{E^{HP,avg}}$ are evaluated against different values of b^{FM}, respectively in Figs. 13 and 14 ($\overline{E^{HP,pk-dp}}$ is excluded as it loses its meaning under DDR). In line with the idea of using DDR on a single-event basis, $\overline{E^{HP,pk}}$ and $\overline{E^{HP,avg}}$ are calculated within the FM window. Additionally, evaluation is performed within the entire second day, to account for potential secondary effects caused by the flexibility provision.

By analysing the trend of $\overline{E^{HP,pk}}$ and $\overline{E^{HP,avg}}$ within the FM window, a saturation behaviour is observed for both KPIs in upwards and downwards flexibility. This is due to the fact that as b^{FM} increases, more flexibility is activated up to a point where technical limitations impede to do it further. In quantitative terms, for upwards flexibility (consumption reduction), peak power within the FM window can be reduced of up to around 20% with mild weather, and around 16% with moderate and heavy weather. Besides, average power can be reduced of up to 35% with mild weather and 30% with moderate and heavy weather. For downwards flexibility (consumption increase), peak power within the DR time window increases of up 100%, 75% and 50%, whereas average power increases of up to 83%, 64% and 51%, for mild, moderate and heavy weather conditions respectively. For downwards flexibility, peak power within the FM window increases of up 100%, 75% and 50% for mild, moderate and heavy weather conditions respectively; average power of up to 83%, 64% and 51%. By extending the KPIs evaluation to the entire second day, it is noted that the provision of upwards flexibility causes an undesired increase of peak power, which is due to the tank pre-charge (see Fig. 11). The worst-case condition is reached for $b^{FM} = 2$, with an increase

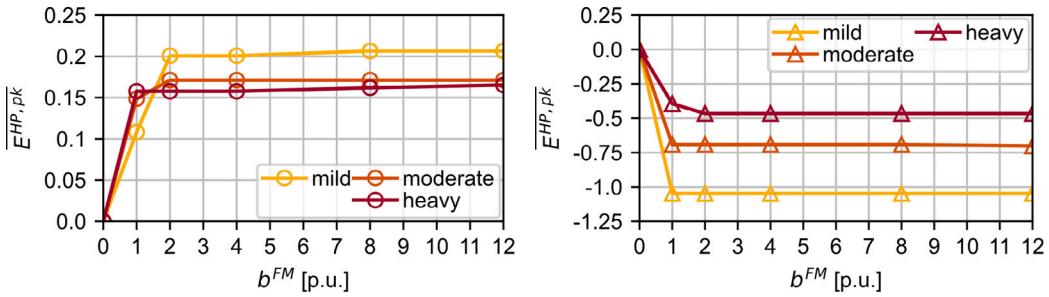

(a) upwards flexibility, market window (b) downwards flexibility, market window

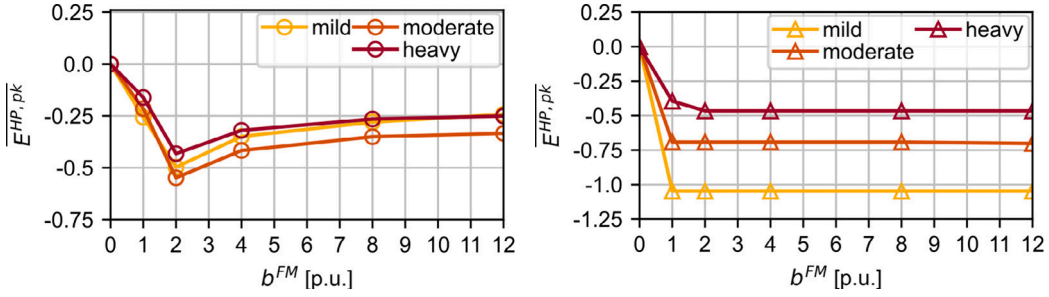

(c) upwards flexibility, second day (d) downwards flexibility, second day

Fig. 13. DDR, $\overline{E^{HP,pk}}$ vs. b^{FM}.

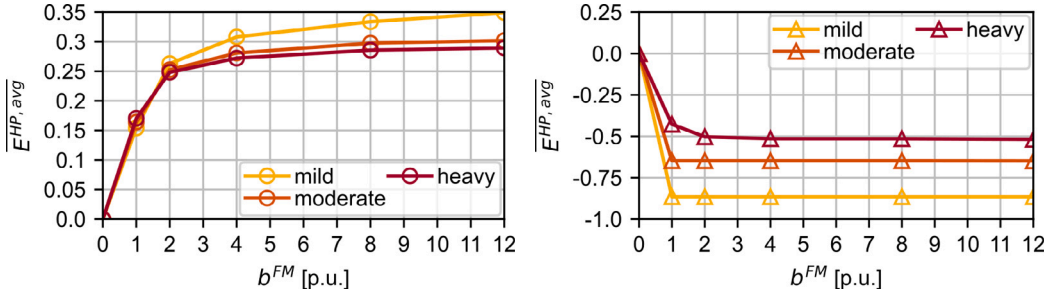

(a) upwards flexibility, market window (b) downwards flexibility, market window

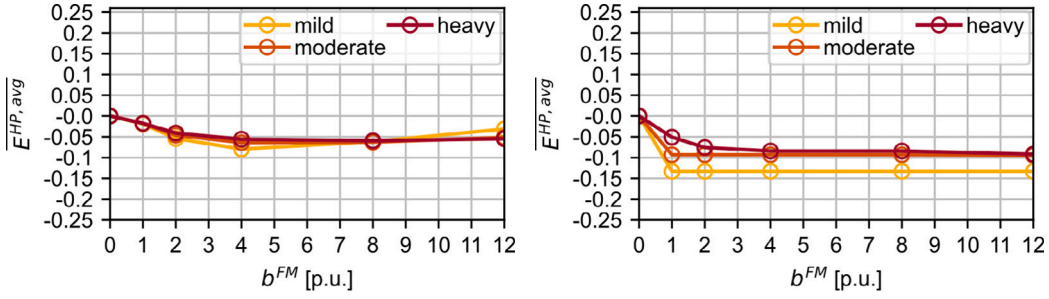

(c) upwards flexibility, second day (d) downwards flexibility, second day

Fig. 14. DDR, $\overline{E^{HP,avg}}$ vs. b^{FM}.

of 50% reached for mild and moderate weather. On the other hand, increase in average power is negligible (lower than 10%), regardless of weather conditions. No relevant secondary effects are incurred for downwards flexibility. This outcome highlights the necessity of accounting for potential undesirable secondary effects when defining a FM windows, including countermeasures such as economic penalties. In terms of optimal scheduling algorithm, possible mitigating actions are the introduction of additional constraints or penalties in the OF.

Finally, $\overline{TEC^{DDR}}$ vs. b^{FM} curves are plotted in Fig. 15. As expected, only positive results are obtained. Here, the key point to observe is that initially $\overline{TEC^{DDR}}$ increases more than linearly, as an increase in b_{FM} induces both a reduction in TEC as well as an increase in flexibility. Then, the trend becomes linear as soon as technical limitations impede to extract flexibility further. For upwards flexibility, TEC reduces at a rate of 2.5%–3.75% with respect to b_{FM}, with no significant difference between weather conditions. For downwards flexibility, TEC reduction rates with respect to b_{FM} are of 40%, 30% and 25%, under respectively mild, moderate and heavy weather conditions.

5.3. Considerations about quality of service and users' comfort

Users comfort preservation rises reasonable concerns when DR programs are implemented through electro-thermal devices such as HP. This aspect is indeed critical in user-level heating systems with a

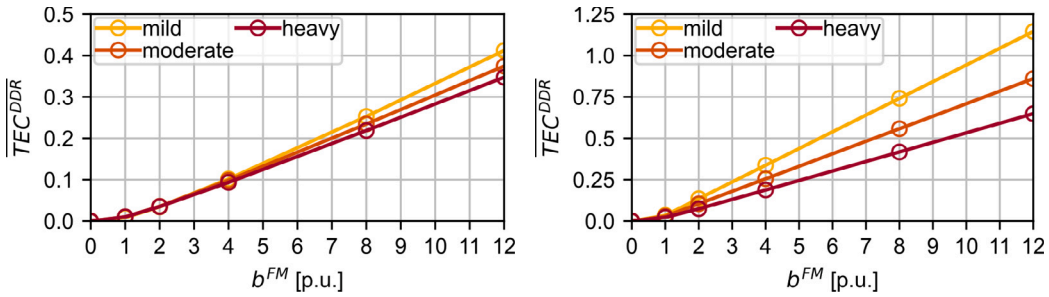

(a) upwards flexibility (b) downwards flexibility

Fig. 15. DDR, $\overline{TEC^{DDR}}$ vs. b^{FM}.

direct coupling between HP and heating elements, e.g., radiators, since DR requires ambients pre-heating, assuming that thermal inertia and insulation suffice to maintain indoor ambient temperature within a comfort range for the occupancy time.

By contrast, in DHS it is not straightforward to directly couple the operation of the central HPs and users comfort, as primary hot water usually does not enter directly the heating elements. For example, users may re-heat primary hot water, mix it with user-produced hot water (e.g., by STCs), or use additional heating sources or heat exchangers that modulate temperature and mass flow rate. Hence, indoor ambient temperature cannot be taken as figures of merit to assess comfort disruptions caused by DR events. On the other hand, comfort disruption may be assessed by means of the quality of service. To this end, it is possible to keep as figure of merit the temperature of the hot water leaving the mixing valve, i.e., T^{us} (see Fig. 2). Indeed, if T^{us} remains unvaried in a DR event, the behaviour of the downstream network would remain unvaried, and so would users' comfort conditions.

In the QP model proposed in this work, T^{us} is assumed to be constant under the widely-adopted hypothesis of ideal control system (see Section 2). In practical terms, the idea is that the control system response time is negligible compared to the DR events duration, so that the desired T^{us} is re-established almost immediately. To the best of the Authors' knowledge, aspects related to control systems are not addressed in research works focusing on energy flows optimisation, as they belong to a different research field and hence are covered in other works [29]. Nonetheless, for the sake of completeness, response of the system considered in this work (see Fig. 2) to DR events is verified in Appendix C through continuous-time simulations with the Open-Modelica software [61].

6. Conclusion

This work proposed a novel formulation of the optimal scheduling problem of district-level HPs, conceived for EMS implementation and aimed at the provision of flexibility services in IDR and DDR programs. Furthermore, a rigorous methodology has been defined to assess the HPs performance under both types of DR. The proposed optimal scheduling has been implemented in a practical case study, where EMS responses under IDR and DDR have been assessed in with mild, moderate and weather conditions. The following key conclusions can be drawn:

- The optimisation problem presents no boolean variables and is of the QP type, and hence solvable through commercially available software.
- Results under IDR prove the capability of providing peak shaving and valley filling services with the EMS set to minimise total energy costs.
- IDR obtained reductions in consumption peak of up to 13% and in peak-to-dip gap of up to 34%.
- Comparison of two IDR price signals proven the possibility of providing flexibility services without extra costs for the end users.
- Under DDR, peak and average consumption follow a saturating trend against increasing flexibility price offers, as no more flexibility can be delivered further to specific prices.
- DDR obtained reductions in peak and average consumption within the FM window of up to respectively 20% and 35% for upwards flexibility, and increases of to 100% and 80% for downwards flexibility. Total energy cost increases against the flexibility price offer at rates of up to 3.75% in upwards and 11.25% in downwards flexibility.
- EMS response to upwards flexibility in DDR yielded an undesired increases of peak consumption outside the FM window of up to 50%, highlighting the need to account for this type of secondary effects.

Future works will revolve around the implementation of the proposed optimisation algorithm into a complete EMS with demand and price forecasting algorithms and based on a rolling time horizon strategy, as well as the joint optimisation of HP with other district-level devices such as BESSs, EVs or PVs.

CRediT authorship contribution statement

Roberto Rocca: Writing – review & editing, Writing – original draft, Visualization, Validation, Software, Resources, Project administration, Methodology, Investigation, Formal analysis, Data curation, Conceptualization. **Stefano Leonori:** Writing – review & editing, Writing – original draft, Supervision, Resources, Project administration, Methodology, Investigation, Formal analysis, Conceptualization. **Gregorio Fernández Aznar:** Validation, Supervision, Resources, Project administration, Funding acquisition. **Riccardo Toffanin:** Validation, Resources, Project administration, Formal analysis, Data curation. **Luis Luengo-Baranguan:** Validation, Supervision, Software, Resources, Project administration, Formal analysis, Data curation.

Declaration of competing interest

The authors declare the following financial interests/personal relationships which may be considered as potential competing interests: Roberto Rocca reports financial support was provided by European Commission. If there are other authors, they declare that they have no known competing financial interests or personal relationships that could have appeared to influence the work reported in this paper.

Acknowledgements

This work has been developed within the framework of the REEFLEX Project - REplicable, interoperable, cross-sector solutions and Energy services for demand side FLEXibility markets, which has received funding from the European Union's Horizon Europe Research and Innovation programme under Grant Agreement No 101096192. This output reflects only the authors' view, and the European Union cannot be held responsible for any use that may be made of the information contained therein.

Table A.5
CoP vs. X^{HP} vs. T^{HP} experimental data.

		X^{HP}									
		0.1	0.2	0.3	0.4	0.5	0.6	0.7	0.8	0.9	1
T^{HP} [°C]	38	5.225	6.618	6.869	7.104	6.948	6.795	6.581	6.385	6.157	6.013
	43	4.426	5.096	5.475	5.793	5.712	5.641	5.481	5.335	5.164	5.06
	48	3.737	3.892	4.354	4.691	4.685	4.674	4.556	4.45	4.322	4.255

Table A.6
CoP interpolation error analysis.

	LLLL Linear	2nd-Order	3rd-Order
RMSE $[kW_{el}/kW_{th}]$	0.015	0.006	0.003
MAPE [%]	6.61	3.08	1.18
max. [%]	12.41	8.39	6.42
min. [%]	−15.77	−6.72	−4.20

Table A.7
Second-order polynomial coefficients for the inverse CoP interpolation.

a_1	0.00016	a_2	−0.0026	a_3	0.181
a_4	−0.0050	a_5	−0.104	a_6	0.153

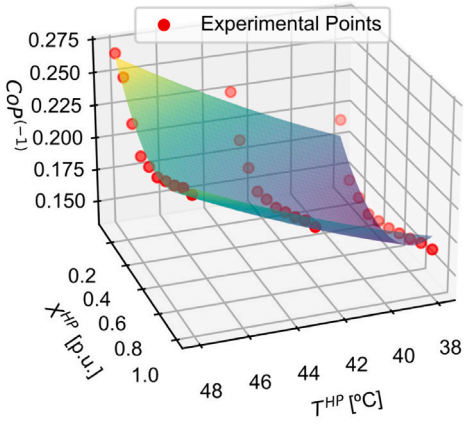

Fig. A.16. Interpolated inverse CoP.

Appendix A. CoP modelling

For large water-to-water HPs, as it is the case in this work, CoP can be expressed as a function of X^{HP} and T^{HP}. For the implementation of the case study of this work, a set of experimental data have been taken from a HP rated at $1245kW_{th}$ from the *York* manufacturer [62], which is reported in Table A.5. Then, different two-variable interpolation techniques have been analysed, namely: linear, second-order, and third-order polynomial.

Accuracy of the three interpolation techniques are compared in Table A.6, where Root Mean Squared Error (RMSE), Mean Average Percent Error (MAPE) and maximum and minimum percent errors are shown.

Provided that the HP optimal scheduling problem formulated in Sections 2 and 3 is of the QP type, accuracy improvement attained with a third-order polynomial would not justify the increase in mathematical complexity and computation time. Therefore, a second-order polynomial is chosen. Inverse of the CoP obtained with a second-order interpolation is plotted in Fig. A.16, while coefficients are reported in Table A.7.

Appendix B. Derivation of (11)

This Appendix provides the mathematical derivation of (11). For ease of reading, (1), (2), (9) and (10) are rewritten and re-numbered. In (B.2), U_k^{HP} is directly expressed as $X_k^{HP}U^{HP,rat}$ (see (3)):

$$U_k^{us} = \mu_k^{us} c_p (T^{us} - T^{ret}). \tag{B.1}$$

$$X_k^{HP}U^{HP,rat} = \mu_k^{HP} c_p \left(T_k^{HP} - T^{ret}\right). \tag{B.2}$$

$$\mu_k^{HP} + \mu_k^{mix} = \mu_k^{us}. \tag{B.3}$$

$$\mu_k^{HP} c_p T_k^{tk} + \mu_k^{mix} c_p T^{ret} = \mu_k^{us} c_p T^{us}. \tag{B.4}$$

Firstly, μ_k^{mix} is extracted from (B.3) and substituted into (B.4). Then, by factoring out terms with μ_k^{HP} and μ_k^{us}, one obtains:

$$\mu_k^{HP} c_p \left(T_k^{tk} - T^{ret}\right) - \underbrace{\mu_k^{us} c_p \left(T_k^{us} - T^{ret}\right)}_{U_k^{us}}. \tag{B.5}$$

Subsequently, $\mu_k^{HP} c_p$ is taken from (B.2) and plugged into (B.5):

$$\frac{X_k^{HP}U^{HP,rat}}{\left(T_k^{HP} - T^{ret}\right)} \left(T_k^{tk} - T^{ret}\right) = U_k^{us}. \tag{B.6}$$

Finally, T_k^{HP} is attained from (B.6):

$$T_k^{HP} = \frac{X_k^{HP}U^{HP,rat}}{U_k^{us}} \left(T_k^{tk} - T^{ret}\right) + T^{ret}. \tag{B.7}$$

Appendix C. Quality of service verification

As discussed in Section 5.3, verification of the quality of service under DR events requires to verify that the control system can re-establish T^{us} almost immediately. As also stated in Section 5.3, control system aspects are normally addressed in separate works. Hence, the Modelica model being presented and shown in Fig. C.17 has been developed with a reasonable compromise between accuracy and simplicity, with the control system relying on two PI controllers. More detailed modelling and advanced control systems are left to future works. It is noted that a mass-flow-controlled pump has been used in lieu of the mixing valve, as it enhances numerical stability and simplifies initialisation, while maintaining the same mass flow control. Simulations have been run with time steps of $0.5s$ with *CVODE* solver.

T^{us} vs. time profiles obtained with simulations are plotted in Fig. C.18, where each spike corresponds to the system response to a different time step. Subplots (a) to (c) represent IDR scenarios, while subplots (d) and (e) represent DDR scenarios. As it can be seen, T^{us} is practically constant, as it ranges between 39.6 °C and 40.1 °C, demonstrating the validity of the ideal control system hypothesis and hence ensuring that quality of service is not affected by DR events. It is reminded that development of a specific control system for the proposed energy flow optimisation algorithm will be addressed in future research works, which will include more detailed system modelling.

Data availability

The authors do not have permission to share data.

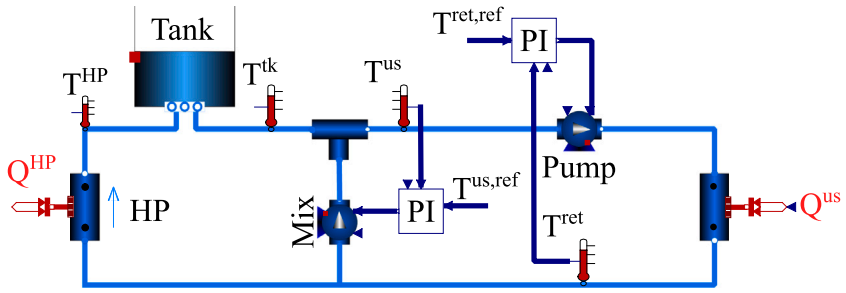

Fig. C.17. System model in Open-Modelica.

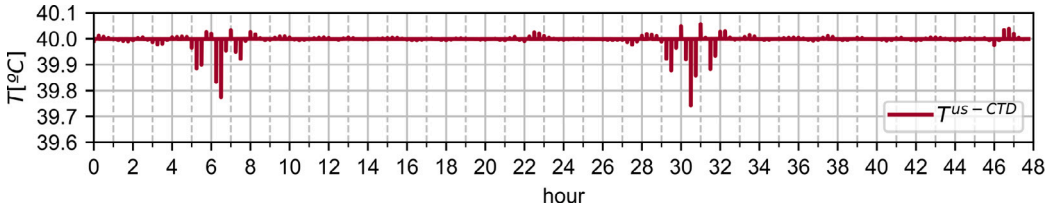

(a) IDR-A

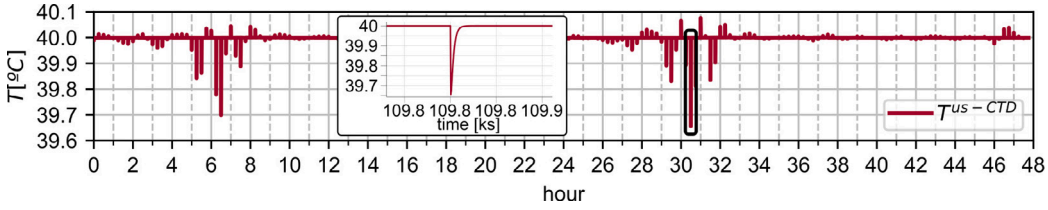

(b) IDR-B

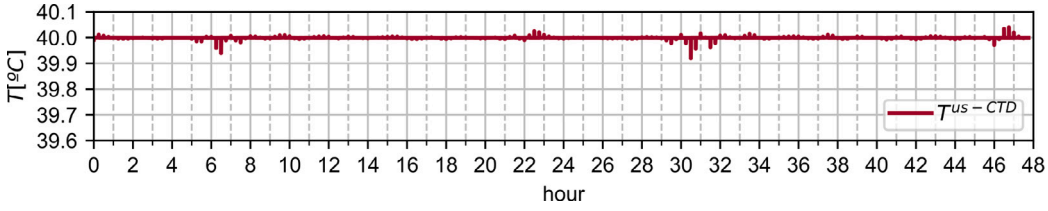

(c) FT

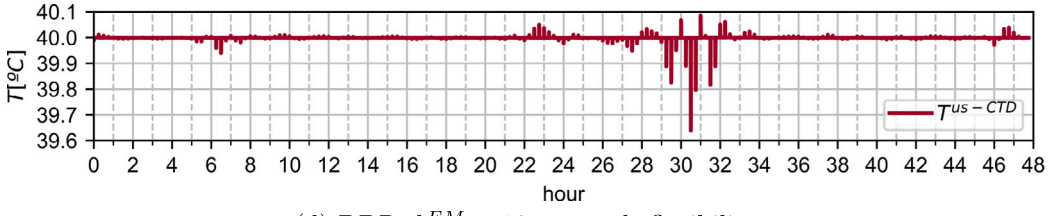

(d) DDR, $b^{FM} = 10$, upwards flexibility

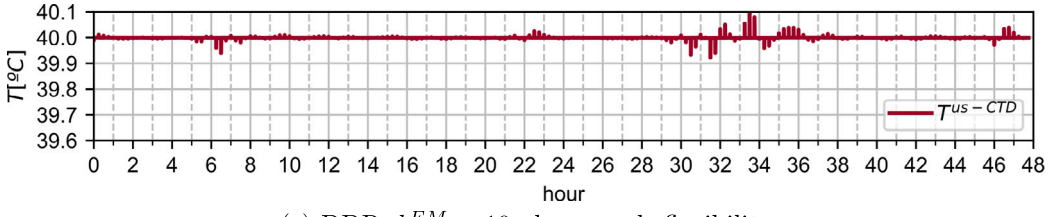

(e) DDR, $b^{FM} = 10$, downwards flexibility

Fig. C.18. T^{us} vs. time profiles in IDR and DDR in continuous-time simulation.

References

[1] Commission E. European green deal. 2019, URL https://commission.europa.eu/strategy-and-policy/priorities-2019-2024/european-green-deal_en.

[2] Morales-España G, Martínez-Gordón R, Sijm J. Classifying and modelling demand response in power systems. Energy 2022;242:122544. http://dx.doi.org/10.1016/j.energy.2021.122544.

[3] Chantzis G, Papadopoulos AM, Giama E, Nizetic S. The potential of demand response as a tool for decarbonization in the energy transition. Energy Build 2023;113255. http://dx.doi.org/10.1016/j.enbuild.2023.113255.

[4] Surve SP, Rocca R, Engeveld EJ, Martínez D, Comech MP, Rivas DM. Impact assessment of different battery energy storage technologies in distribution grids with high penetration of renewable energies. Renew Energy Power Qual J (RE& pqJ) 2022;20:650–5. http://dx.doi.org/10.24084/repqj20.391.

[5] Menéndez-Agudín A, Rocca R, Fernández G, Luengo-Baranguán L, Zaldivar D. Hydrogen technologies to provide flexibility to the electric system: A review. Renew Energy Power Qual J (RE& pqJ) 2022;20:656–61. http://dx.doi.org/10.24084/repqj20.392.

[6] Rocca R, Papadopoulos S, Rashed M, Prassinos G, Giulii Capponi F, Galea M. A one-body, laminated-rotor flywheel switched reluctance machine for energy storage: Design trade-offs. In: 2020 IEEE international conference on environment and electrical engineering and 2020 IEEE industrial and commercial power systems europe. IEEE; 2020, p. 1–6. http://dx.doi.org/10.1109/EEEIC/ICPSEurope49358.2020.9160512.

[7] Bernal-Sancho M, Paz Comech M, Galán-Hernández N. Damping control in renewable-integrated power systems: A comparative analysis of PSS, POD-P, and POD-Q strategies. Int J Electr Power Energy Syst 2024;162:110308. http://dx.doi.org/10.1016/j.ijepes.2024.110308.

[8] Girona-Badia J, Lacerda VA, Spier DW, Prieto-Araujo E, Gomis-Bellmunt O. Resource-aware grid-forming synchronization control: Design, analysis and validation. IEEE Trans Energy Convers 2024;1–12. http://dx.doi.org/10.1109/TEC.2024.3486056.

[9] O'Connell N, Pinson P, Madsen H, O'Malley M. Benefits and challenges of electrical demand response: A critical review. Renew Sustain Energy Rev 2014;39:686–99. http://dx.doi.org/10.1016/j.rser.2014.07.098.

[10] Striani S, Unterluggauer T, Andersen PB, Marinelli M. Flexibility potential quantification of electric vehicle charging clusters. Sustain Energy Grids Netw. 2024;101547. http://dx.doi.org/10.1016/j.segan.2024.101547.

[11] Shen F, Wu Q, Jin X, Zhang M, Teimourzadeh S, Tor OB. Coordination of dynamic tariff and scheduled reprofiling product for day-ahead congestion management of distribution networks. Int J Electr Power Energy Syst 2022;135:107612. http://dx.doi.org/10.1016/j.ijepes.2021.107612.

[12] Zhang C, Wang Q, Wang J, Korpås M, Khodayar ME. Strategy-making for a proactive distribution company in the real-time market with demand response. Appl Energy 2016;181:540–8. http://dx.doi.org/10.1016/j.apenergy.2016.08.058.

[13] Council of European Union. Directive (EU) 2019/944 of the European parliament and of the council of 5 june 2019 on common rules for the internal market for electricity and amending directive 2012/27/EU. 2019, https://eur-lex.europa.eu/eli/dir/2019/944/oj.

[14] Piclo. 2024, URL https://www.piclo.energy/.

[15] Bloess A, Schill W-P, Zerrahn A. Power-to-heat for renewable energy integration: A review of technologies, modeling approaches, and flexibility potentials. Appl Energy 2018;212:1611–26. http://dx.doi.org/10.1016/j.apenergy.2017.12.073.

[16] Fambri G, Mazza A, Guelpa E, Verda V, Badami M. Power-to-heat plants in district heating and electricity distribution systems: A techno-economic analysis. Energy Convers Manage 2023;276:116543. http://dx.doi.org/10.1016/j.enconman.2022.116543.

[17] Badami M, Fambri G. Optimising energy flows and synergies between energy networks. Energy 2019;173:400–12. http://dx.doi.org/10.1016/j.energy.2019.02.007.

[18] Santamouris M, Vasilakopoulou K. Present and future energy consumption of buildings: Challenges and opportunities towards decarbonisation. E- Prime - Adv Electr Eng Electron Energy 2021;1:100002. http://dx.doi.org/10.1016/j.prime.2021.100002.

[19] International Energy Agency (IEA). URL https://www.iea.org/energy-system/buildings/heating.

[20] Guelpa E, Verda V. Demand response and other demand side management techniques for district heating: A review. Energy 2021;219:119440. http://dx.doi.org/10.1016/j.energy.2020.119440.

[21] Pavičević M, Mangipinto A, Nijs W, Lombardi F, Kavvadias K, Jiménez Navarro JP, Colombo E, Quoilin S. The potential of sector coupling in future European energy systems: Soft linking between the dispa-SET and JRC-EU-TIMES models. Appl Energy 2020;267:115100. http://dx.doi.org/10.1016/j.apenergy.2020.115100.

[22] Jiang Y, Wan C, Botterud A, Song Y, Xia S. Exploiting flexibility of district heating networks in combined heat and power dispatch. IEEE Trans Sustain Energy 2020;11(4):2174–88. http://dx.doi.org/10.1109/TSTE.2019.2952147.

[23] Rocca R, Elorza-Uriarte L, Schamhart A, Verschuur G, Rivas-Ascaso DM. Electrical flexibility forecasting and assessment for heat-pump-based district heating systems. In: 2024 IEEE international conference on environment and electrical engineering and 2024 IEEE industrial and commercial power systems europe. 2024, p. 1–6. http://dx.doi.org/10.1109/EEEIC/ICPSEurope61470.2024.10751082.

[24] Rocca R, Elorza-Uriarte L, Zubia I, Farrace D, Toffanin R, Rivas-Ascaso DM. Techno-economic analysis of electrical flexibility in combustion-based district heating systems: A swiss case study. Int J Electr Power Energy Syst 2024;157:109869. http://dx.doi.org/10.1016/j.ijepes.2024.109869.

[25] Golmohamadi H, Larsen KG, Jensen PG, Hasrat IR. Integration of flexibility potentials of district heating systems into electricity markets: A review. Renew Sustain Energy Rev 2022;159:112200. http://dx.doi.org/10.1016/j.rser.2022.112200.

[26] Romero Rodríguez L, Sánchez Ramos J, Álvarez Domínguez S, Eicker U. Contributions of heat pumps to demand response: A case study of a plus-energy dwelling. Appl Energy 2018;214:191–204. http://dx.doi.org/10.1016/j.apenergy.2018.01.086.

[27] Leonori S, Martino A, Frattale Mascioli FM, Rizzi A. Microgrid energy management systems design by computational intelligence techniques. Appl Energy 2020;277:115524. http://dx.doi.org/10.1016/j.apenergy.2020.115524.

[28] Li H, Wang Z, Hong T, Piette MA. Energy flexibility of residential buildings: A systematic review of characterization and quantification methods and applications. Adv Appl Energy 2021;3:100054. http://dx.doi.org/10.1016/j.adapen.2021.100054.

[29] Blaud PC, Haurant P, Claveau F, Lacarrière B, Chevrel P, Mouraud A. Modelling and control of multi-energy systems through multi-prosumer node and economic model predictive control. Int J Electr Power Energy Syst 2020;118:105778. http://dx.doi.org/10.1016/j.ijepes.2019.105778.

[30] Abokersh MH, Saikia K, Cabeza LF, Boer D, Vallès M. Flexible heat pump integration to improve sustainable transition toward 4th generation district heating. Energy Convers Manage 2020;225:113379. http://dx.doi.org/10.1016/j.enconman.2020.113379.

[31] Bahlawan H, Castorino GAM, Losi E, Manservigi L, Spina PR, Venturini M. Optimal management with demand response program for a multi-generation energy system. Energy Convers Manag: X 2022;16:100311. http://dx.doi.org/10.1016/j.ecmx.2022.100311.

[32] Bahlawan H, Morini M, Pinelli M, Spina PR, Venturini M. Optimization of energy and economic scheduling of a hybrid energy plant by using a dynamic programming approach. Appl Therm Eng 2021;187:116577. http://dx.doi.org/10.1016/j.applthermaleng.2021.116577.

[33] Ayele GT, Mabrouk MT, Haurant P, Laumert B, Lacarrière B. Optimal heat and electric power flows in the presence of intermittent renewable source, heat storage and variable grid electricity tariff. Energy Convers Manage 2021;243:114430. http://dx.doi.org/10.1016/j.enconman.2021.114430.

[34] Bischi A, Taccari L, Martelli E, Amaldi E, Manzolini G, Silva P, Campanari S, Macchi E. A detailed MILP optimization model for combined cooling, heat and power system operation planning. Energy 2014;74:12–26. http://dx.doi.org/10.1016/j.energy.2014.02.042.

[35] Zhang M, Wu Q, Wen J, Zhou B, Guan Q, Tan J, Lin Z, Fang F. Day-ahead stochastic scheduling of integrated electricity and heat system considering reserve provision by large-scale heat pumps. Appl Energy 2022;307:118143. http://dx.doi.org/10.1016/j.apenergy.2021.118143.

[36] Moretti L, Martelli E, Manzolini G. An efficient robust optimization model for the unit commitment and dispatch of multi-energy systems and microgrids. Appl Energy 2020;261:113859. http://dx.doi.org/10.1016/j.apenergy.2019.113859.

[37] Moretti L, Manzolini G, Martelli E. MILP and MINLP models for the optimal scheduling of multi-energy systems accounting for delivery temperature of units, topology and non-isothermal mixing. Appl Therm Eng 2021;184:116161. http://dx.doi.org/10.1016/j.applthermaleng.2020.116161.

[38] Ghilardi LMP, Castelli AF, Moretti L, Morini M, Martelli E. Co-optimization of multi-energy system operation, district heating/cooling network and thermal comfort management for buildings. Appl Energy 2021;302:117480. http://dx.doi.org/10.1016/j.apenergy.2021.117480.

[39] Wang H, Han J, Zhang R, Sun M, Sun Z, Hua P, Xie Z, Wang H, Abdollahi E, Lahdelma R, Granlund K, Teppo E. Heat-power peak shaving and wind power accommodation of combined heat and power plant with thermal energy storage and electric heat pump. Energy Convers Manage 2023;297:117732. http://dx.doi.org/10.1016/j.enconman.2023.117732.

[40] EnergyPRO. URL https://www.emd-international.com/energypro/.

[41] Simonetti R, Moretti L, Molinaroli L, Manzolini G. Energetic and economic optimization of the yearly performance of three different solar assisted heat pump systems using a mixed integer linear programming algorithm. Energy Convers Manage 2020;206:112446. http://dx.doi.org/10.1016/j.enconman.2019.112446.

[42] Langer L, Volling T. An optimal home energy management system for modulating heat pumps and photovoltaic systems. Appl Energy 2020;278:115661. http://dx.doi.org/10.1016/j.apenergy.2020.115661.

[43] Salpakari J, Lund P. Optimal and rule-based control strategies for energy flexibility in buildings with PV. Appl Energy 2016;161:425–36. http://dx.doi.org/10.1016/j.apenergy.2015.10.036.

[44] Salpakari J, Rasku T, Lindgren J, Lund PD. Flexibility of electric vehicles and space heating in net zero energy houses: an optimal control model with thermal dynamics and battery degradation. Appl Energy 2017;190:800–12. http://dx.doi.org/10.1016/j.apenergy.2017.01.005.
[45] Dengiz T, Jochem P, Fichtner W. Demand response with heuristic control strategies for modulating heat pumps. Appl Energy 2019;238:1346–60. http://dx.doi.org/10.1016/j.apenergy.2018.12.008.
[46] Clauß J, Stinner S, Sartori I, Georges L. Predictive rule-based control to activate the energy flexibility of norwegian residential buildings: Case of an air-source heat pump and direct electric heating. Appl Energy 2019;237:500–18. http://dx.doi.org/10.1016/j.apenergy.2018.12.074.
[47] Wu X, Li Y, Tan Y, Cao Y, Rehtanz C. Optimal energy management for the residential MES. IET Gener Transm Distrib 2019;13(10):1786–93.
[48] Efkarpidis NA, Vomva SA, Christoforidis GC, Papagiannis GK. Optimal day-to-day scheduling of multiple energy assets in residential buildings equipped with variable-speed heat pumps. Appl Energy 2022;312:118702. http://dx.doi.org/10.1016/j.apenergy.2022.118702.
[49] Zhang T, Parisio A. Distributed control of flexible assets in distribution networks considering personal usage plans. Sustain Energy Grids Netw. 2025;42:101638. http://dx.doi.org/10.1016/j.segan.2025.101638.
[50] HE Project REEFLEX. URL https://reeflexhe.eu/.
[51] International Energy Agency (IEA). URL https://www.iea.org/energy-system/buildings/district-heating.
[52] Lund H, Werner S, Wiltshire R, Svendsen S, Thorsen JE, Hvelplund F, Mathiesen BV. 4Th generation district heating (4GDH): Integrating smart thermal grids into future sustainable energy systems. Energy 2014;68:1–11. http://dx.doi.org/10.1016/j.energy.2014.02.089.
[53] Saletti C, Gambarotta A, Morini M. Development, analysis and application of a predictive controller to a small-scale district heating system. Appl Therm Eng 2020;165:114558. http://dx.doi.org/10.1016/j.applthermaleng.2019.114558.
[54] Yousefi S, Moghaddam MP, Majd VJ. Optimal real time pricing in an agent-based retail market using a comprehensive demand response model. Energy 2011;36(9):5716–27. http://dx.doi.org/10.1016/j.energy.2011.06.045.
[55] Kuivjõgi H, Vasman S, Petlenkov E, Thalfeldt M, Kurnitski J. Data-driven baseline generation for post-retrofit energy saving assessment, a comparison of statistical and machine learning methods. J Build Eng 2024;98:111016. http://dx.doi.org/10.1016/j.jobe.2024.111016.
[56] CVXOPT. URL https://cvxopt.org/.
[57] GAMS. URL https://www.gams.com/.
[58] GUROBI. URL https://www.gurobi.com/.
[59] Capriasca Calore, l'impianto di teleriscaldamento della Capriasca. URL http://www.capriascacalore.ch/.
[60] Nussbaumer T, Thalmann S, Ardens AJ, Ködel J. Handbook on Planning of District Heating Networks. Bern: Swiss Federal Office of Energy; 2020.
[61] OpenModelica. URL https://openmodelica.org/.
[62] York. URL https://www.york.com/.